

Synergetic Community Search over Large Multilayer Graphs

Chengyang Luo
Zhejiang University
Hangzhou, China
luocy1017@zju.edu.cn

Qing Liu
Zhejiang University
Hangzhou, China
qingliucs@zju.edu.cn

Yunjun Gao
Zhejiang University
Hangzhou, China
gaoyj@zju.edu.cn

Jianliang Xu
Hong Kong Baptist University
Hong Kong, China
xujl@comp.hkbu.edu.hk

ABSTRACT

Community search is a fundamental problem in graph analysis and has attracted much attention for its ability to discover personalized communities. In this paper, we focus on community search over multilayer graphs. We design a novel cohesive subgraph model called *synergetic core* for multilayer graphs, which requires both *local* and *global* cohesiveness. Specifically, the synergetic core mandates that the vertices within the subgraph are not only densely connected on some individual layers but also form more cohesive connections on the projected graph that considers all layers. The local and global cohesiveness collectively ensure the superiority of the synergetic core. Based on this new model, we formulate the problem of *synergetic community search*. To efficiently retrieve the community, we propose two algorithms. The first is a progressive search algorithm, which enumerates potential layer combinations to compute the synergetic core. The second is a *trie-based search algorithm*, leveraging our novel index called *dominant layers-based trie* (DLT). DLT compactly stores synergetic cores within the trie structure. By traversing the DLT, we can efficiently identify the synergetic core. We conduct extensive experiments on nine real-world datasets. Experimental results demonstrate that (1) the synergetic core can find communities with the best quality among the state-of-the-art models, and (2) our proposed algorithms are up to five orders of magnitude faster than the basic method.

PVLDB Artifact Availability:

The source code, data, and/or other artifacts have been made available at <https://github.com/ZJU-DAILY/SynCore>.

1 INTRODUCTION

Real-world graphs, such as social networks [2], financial networks [9], and biological networks [21], often encompass multiple types of relationships between entities. Multilayer graphs, denoted by $G = (V, E, L)$, can effectively model such graphs with different types of relationships [13]. Specifically, in G , the vertex set V is consistent across all layers in L , with edges on different layers representing different types of relationships. Figure 1 illustrates a multilayer graph G which is composed of three layers.

Community search, an important tool for graph analysis, aims to find a cohesive subgraph that includes a specified set of query vertices [16, 25, 33, 42]. Prior research has extensively explored community search across various graph types, such as bipartite graphs [49], directed graphs [17, 38], temporal graphs [32, 35], and

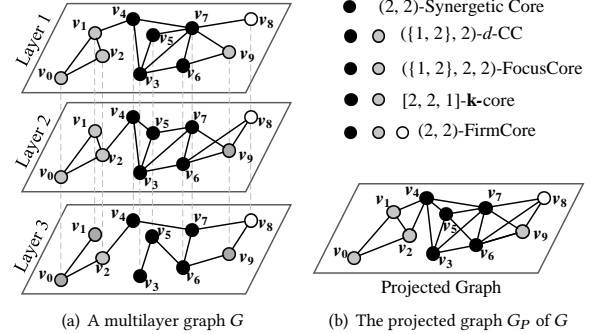


Figure 1: An example of the multilayer graph

heterogeneous information networks [18, 27]. In this paper, we focus on community search over multilayer graphs [4].

The cohesiveness is a crucial metric for community search [16, 25, 45]. To identify cohesively connected communities, numerous cohesive subgraph models have been proposed, including k -core [43], k -truss [26], and k -clique [10]. The k -core model, in particular, has attracted significant attention for its computational efficiency and effectiveness in identifying densely connected communities. Several core-based cohesive subgraph models tailored for multilayer graphs have also been proposed, such as k -core [19], d -CC [36, 53], FirmCore [20], and FocusCore [50]. Specifically, a k -core with $\mathbf{k} = [k_1, k_2, \dots, k_{|L|}]$ requires that each vertex in the k -core has at least k_l neighbors on layer $l \in L$. A d -CC, given an integer d and a layer set $L' \subseteq L$, is a subgraph where every vertex connects to at least d neighbors on each layer $l \in L'$. For the FirmCore, given parameters k and λ , every vertex is connected to no less than k neighbors across at least λ layers, with the specific layers varying per vertex. The FocusCore integrates elements of d -CC and FirmCore, taking three parameters: $(\mathcal{F}, k, \lambda)$. In a $(\mathcal{F}, k, \lambda)$ -FocusCore, each vertex has (1) at least k neighbors on each layer in \mathcal{F} , and (2) at least k neighbors across a minimum of λ layers.

However, existing core-based models for multilayer graphs have several limitations. First, models like k -core, d -CC, and FocusCore require users to set multiple parameters, such as specifying k_l for each layer $l \in L$ in k -core or selecting layers that meet degree constraints in d -CC and FocusCore. This can be a challenge, especially for users unfamiliar with the graph's structure. Second, while FirmCore simplifies parameter settings, it often produces the least cohesive communities, as it does not require a k -core structure within any individual layer. Last but not least, all existing models focus primarily on local cohesiveness within layers, neglecting the crucial concept of *global cohesiveness* in multilayer graphs. Specifically, a set of vertices may form dense subgraphs on particular layers. However, when all layers are considered concurrently, these vertices may constitute an even denser subgraph, which could lead to the discovery of a significantly more cohesive community.

This work is licensed under the Creative Commons BY-NC-ND 4.0 International License. Visit <https://creativecommons.org/licenses/by-nc-nd/4.0/> to view a copy of this license. For any use beyond those covered by this license, obtain permission by emailing info@vldb.org. Copyright is held by the owner/author(s). Publication rights licensed to the VLDB Endowment.

Proceedings of the VLDB Endowment, Vol. 14, No. 1 ISSN 2150-8097.
doi:XX.XX/XXX.XX

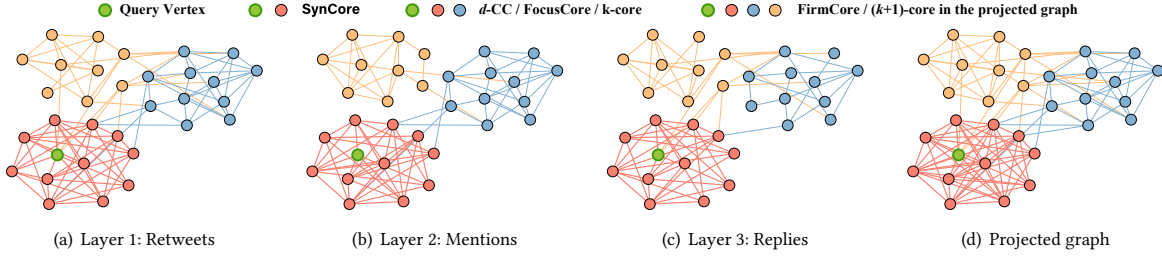


Figure 2: Case study on Twitter

To address these limitations, we propose a new cohesive subgraph model called *synergetic core* (SynCore), which requires that the subgraph is not only dense within individual layers but also exhibits greater cohesion across all layers. Notably, as observed in our experiments, if we consider only local or global cohesiveness, the resulting communities show inferior densities, confirming the necessity of taking both local and global cohesiveness into account simultaneously. To this end, we employ the concept of *projected graph* to represent the global aspect of a multilayer graph. Specifically, the projected graph G_P of a multilayer graph G is a simple, single-layer graph that shares the same vertex set as G . In G_P , an edge exists between vertices u and v if there is at least one layer of G in which u and v are connected by an edge. Figure 1(b) shows the projected graph of G in Figure 1(a). Based on the projected graph, the SynCore is defined as follows. Given a multilayer graph G , an integer k , and a support threshold $s \in [1, |L|]$, the (k, s) -SynCore is defined as the maximum subgraph $H \subseteq G$ that satisfies: (i) there are at least s layers in which H is a k -core. (ii) in the projected graph of G , H is a k' -core with $k' > k$. Notably, if H is a k -core in some layers, it must also be a k -core in the projected graph. Thus, for condition (ii), we require $k' > k$. We illustrate the advantage of SynCore via a case study on a real-world multilayer graph Twitter [52], as shown in Figure 2. Twitter is a multilayer social network extracted from the Twitter data during the Cannes Film Festival. The graph consists of three layers, each representing a different type of social interaction: retweets, mentions, and replies. The green vertex represents the query vertex. Communities returned by different models consist of vertices of different colors. The community identified by SynCore, consisting of red and green vertices, represents a group of people who frequently interact with each other on the platform, and are likely to share similar film preferences with the query vertex. The advantages of SynCore are twofold. First, the community of SynCore is more cohesive than those returned by other models. Second, SynCore is effective at excluding irrelevant vertices. For example, the blue and yellow vertices, which are not relevant to the query vertex, are contained in the communities returned by other models, but SynCore successfully prunes them. As a result, SynCore is more effective than other models.

Based on SynCore, we systematically study the problem of *synergetic community search* (SynCS) over large multilayer graphs. Specifically, given a query vertex set Q , SynCS aims to find a maximum connected subgraph which contains Q and qualifies as a SynCore. The SynCS problem has diverse applications, such as friend recommendation [7, 25], cooperative team identification [34], and fraud detection [9]. For example, in social networks, multilayer graphs can model user friendships across platforms. SynCS can be used to identify a community in which users not only have strong connections on specific platforms but also demonstrate closer friendships on

the whole. Such a community is more likely to be a group of people with similar interests, thereby enhancing the effectiveness of friend recommendations within the community. As another example, consider transaction networks from different financial institutions, which can be combined into a multilayer graph. SynCS can uncover hidden accounts that frequently transact with a suspicious account across multiple institutions. These accounts show discreetly high activity on individual platforms but trade more frequently overall, potentially indicating a criminal group.

A basic approach for SynCS is to enumerate all possible combinations of s layers and compute the (k, s) -SynCore for each, resulting in $\binom{|L|}{s}$ combinations. However, this process is inefficient. To improve search efficiency, we propose a progressive search algorithm. First, we introduce the Quasi-SynCore, a relaxed version of SynCore, which reduces the graph to a smaller subgraph in linear time. It significantly pruning the search space. Second, we design rules to selectively enumerate layer combinations likely to contain the final result, avoiding exhaustive enumeration. All SynCores in a multilayer graph can be precomputed, allowing more efficient community search. To further accelerate this process, we introduce the *dominant layers-based trie* (DLT). Storing all SynCores is storage-intensive due to the large number of layer combinations, so we propose the concept of *dominant layers*. It represent the maximal set of layers where a vertex v is contained in a SynCore. DLT uses these dominant layers to store only a fraction of SynCores, reducing storage significantly. It organizes these layers in a trie, with each node representing a set of dominant layers and associated vertices. This enables efficient search through DLT for SynCS.

Overall, we make the following contributions in this paper.

- We propose a novel cohesive subgraph model called synergetic core for multilayer graphs. Based on it, we formally define and study the synergetic community search problem.
- We propose a progressive search algorithm for the SynCS problem that greatly prunes the search space and improves search efficiency.
- To further enhance efficiency, we develop an efficient trie-based search algorithm for the SynCS problem by designing a novel index called DLT. Additionally, we propose efficient algorithms to construct and maintain DLT.
- We conduct extensive experimental studies on ten real-world graphs. Experimental results validate the quality of the synergetic core and demonstrate the efficiency of the proposed algorithms.

The rest of this paper is organized as follows. Section 2 reviews related work. Section 3 formally defines the synergetic core and the synergetic community search problem. Section 4 presents the progressive search algorithm. Section 5 proposes Dominant Layers Trie and the DLT-based search algorithm. Experimental results are reported in Section 6. Finally, Section 7 concludes the paper.

2 RELATED WORK

We review the related work from two aspects, including *cohesive subgraph models for multilayer graph*, and *community search*.

Cohesive Subgraph Models for Multilayer Graph. Various core-based cohesive subgraph models have been proposed for multilayer graphs by extending the k -core [43]. The \mathbf{k} -core [19] with a vector $\mathbf{k} = [k_1, k_2, \dots, k_{|L|}]$ requires the identified subgraph on each layer $l \in L$ to be a k_l -core. The d -CC [36, 53] is a d -core on each layer of a given subset $L' \subseteq L$. The FirmCore [20] ensures each vertex has at least k neighbors on at least λ layers. The FocusCore [50] is a combination of d -CC and FirmCore. Moreover, gCore [37] and CrossCore [46] are proposed for the multilayer heterogeneous information graphs by extending the k -core and d -CC, respectively. The multilayer heterogeneous information graph is a variant of the multilayer graph where vertices differ across layers and cross-layer connections exist. Other cohesive models for multilayer graphs include the frequent cross-graph γ -quasi-clique [28], which identifies the subgraph forming a γ -quasi-clique on some layers. The FirmTruss [4] ensures each edge is part of at least $k - 2$ triangles on at least λ layers. The TrussCube [23] finds subgraphs where each edge is part of at least $k-2$ triangles on all layers of L' . Note that SynCore differs from existing models in several key aspects: (i) Unlike models based on truss or clique [4, 23, 28], SynCore is a novel core-based model that is more computationally efficient [16]. (ii) Models such as [37, 46] are tailored for the heterogeneous information graph, whereas SynCore is designed for the standard multilayer graph. (iii) Existing core models [19, 20, 36, 50, 53] focus on local properties on individual layers, while SynCore integrates both local and global cohesiveness, allowing for identifying communities with higher quality.

Community Search. Sozio and Giannis [45] first introduced the community search problem. Since then, various cohesive subgraph models have been proposed for community search over simple graphs, such as k -core [3, 11], k -truss [1, 24, 26], k -clique [10], k -plex [51], and k -ECC [5]. Community search has also been studied for more complex graphs, including directed graphs [17, 38], bipartite graphs [49], keyword-based graphs [15, 39], location-based graphs [6, 14], temporal graphs [32, 35], and heterogeneous information networks [18, 27]. Recently, several learning-based methods have been proposed for community search. QD-GNN [29], AQD-GNN [29], and ALICE [48] address the community search in a supervised manner. COCLEP [31] employs contrastive learning and tackles community search in a semi-supervised manner. TransZero [47] supports unsupervised community search, which trains a graph transformer in a self-supervised manner. However, community search over multilayer graphs has received less attention. Behrouz et al. [4] studied the FirmTruss community search problem. Differing from previous studies on single-layer graphs [3, 5, 11], we focus on multilayer graphs and propose a novel core-based model for community search.

3 PRELIMINARIES

A multilayer graph is denoted by $G = (V, E, L)$, where V , L , and $E \subseteq V \times V \times L$ are the sets of vertices, layers, and edges, respectively. We denote the set of edges on layer l as E_l . For a vertex $v \in V$, if $\exists l \in L, (u, v, l) \in E$, we call u a neighbor of v . Let $N_l(v)$ represent

the neighbors of v on layer l . The degree of vertex v on layer l in G is denoted by $\deg_l^G(v) = |N_l(v)|$. Moreover, for a subset of vertices $H \subseteq V$, $G_l[H]$ denotes the subgraph of G induced by H on layer l .

Definition 3.1. (Projected Graph). Given a multilayer graph $G = (V, E, L)$, the projected graph of G is denoted as $G_P = (V_P, E_P)$, where $V_P = V$, $E_P = \{(u, v) \mid \exists l \in L, (u, v, l) \in E\}$.

According to Definition 3.1, the projected graph G_P of the multilayer graph G is a single-layer graph that shares the same set of vertices as the multilayer graph. The edges in the projected graph are the union of edges from all layers of the multilayer graph. For a vertex $v \in V_P$, $N_P(v)$ represents the neighbors of v in the projected graph. For a set of vertices $H \subseteq V$, $G_P[H]$ denotes the subgraph of G_P induced by H , and $\deg_P^H(v)$ denotes the degree of vertex v in this subgraph. For the sake of simplicity, when the context is clear, we will denote $\deg_l^H(v)$ and $\deg_P^H(v)$ as $\deg_l(v)$ and $\deg_P(v)$, respectively. Based on the multilayer graph and projected graph, we formally define the synergetic core as follows.

Definition 3.2. (Synergetic Core (SynCore)). Given a multilayer graph $G = (V, E, L)$, an integer $k \geq 0$, a support threshold $1 \leq s \leq |L|$, the SynCore of G , denoted by SC_s^k , is a maximal vertex set $H \subseteq V$ satisfying:

- (i) **Local cohesiveness:** there is a set of layers $L' \subseteq L$ with $|L'| \geq s$ such that $\forall v \in H, \forall l \in L', \deg_l^H(v) \geq k$;
- (ii) **Global cohesiveness:** in the projected graph G_P of G , $\forall v \in H, \deg_P^H(v) > k$.

We would like to highlight two points for the SynCore. (1) The local cohesiveness only ensures each vertex v has at least k neighbors in at least s layers, but it does not guarantee all vertices have at least $k + 1$ neighbors in at least s layers. The global cohesiveness helps to prune the vertices that have exactly k neighbors in the projected graph, and thus is not redundant. (2) We use the same k for both local and global cohesiveness to reduce the number of parameters. Actually, the local cohesiveness and global cohesiveness can also be set with different k 's, as long as the global cohesiveness uses a larger k than that used for local cohesiveness.

In the following, if a SynCore forms a k -core on each layer in $L' \subseteq L$, it is denoted by $SC_{L'}^k$.

Differences from Existing Models. First, the most significant difference between SynCore and other models is that SynCore considers both the local (i.e., on individual layers) and global (i.e., in the projected graph) cohesivenesses of multilayer graphs. Second, SynCore only requires two parameters, namely k and s . In contrast, the \mathbf{k} -core model necessitates $|L|$ different parameters, one for each layer; the d -CC and FocusCore require a manual specification of the layers that satisfy the degree requirements. Fewer parameters can relieve users from the burdensome task of setting parameters. Third, unlike FirmCore, SynCore ensures the k -core structure.

Based on SynCore, we formally define the studied problem.

PROBLEM 1. (Synergetic Community Search). Given a multilayer graph $G = (V, E, L)$, an integer $k \geq 0$, a support threshold $1 \leq s \leq |L|$, and a set of query vertices $Q \subseteq V$, the synergetic community search (SynCS) is to find a vertex set $H \subseteq V$ satisfying:

- (i) **Containment:** $Q \subseteq H$;
- (ii) **Cohesiveness:** H is a SynCore;
- (iii) **Connectivity:** H is connected in the projected graph G_P ;
- (iv) **Maximum:** H is maximum.

Example 1. In Figure 1, suppose we set $k = 2$, $s = 2$, and $Q = \{v_5\}$. The black vertices, i.e., $\{v_3, v_4, v_5, v_6, v_7\}$, represent the result of SynCS. These vertices constitute a 2-core on both layer 1 and layer 2, and a 3-core in the projected graph.

A basic method to handle SynCS is to enumerate all possible combinations of s layers. For each layer combination L' , we can employ the peeling method to find SynCore containing the query vertex set, i.e., to iteratively delete the vertices that do not satisfy the degree constraints. Finally, the maximum SynCore is returned. However, this basic method suffers from performance issues. Specifically, for each layer combination L' , computing the SynCore requires $O(|E| + |V|)$ time. Since there are $\binom{L}{s}$ possible layer combinations, the overall time complexity amounts to $O(\binom{L}{s} \cdot (|E| + |V|))$. Clearly, the basic method is inefficient when $\binom{L}{s}$ is large. To address this, we propose more efficient algorithms in Sections 4 and 5.

4 PROGRESSIVE SEARCH ALGORITHM

The basic method should enumerate all layer combinations. Actually, some layer combinations do not contain the SynCore, and thus enumerating them is unnecessary. If we enumerate as few layer combinations as possible, the algorithm's performance will improve. Motivated by it, in this section, we propose a progressive search algorithm (PSA). The basic idea of PSA is to first identify candidate vertices that may contain the SynCore. Then, PSA iteratively enumerates the potential layer combinations for the candidate vertices that may contain the SynCore, and prunes the candidate vertices until the maximum SynCore is found. There are two issues that PSA needs to address. (1) What vertices constitute the candidate vertices? (2) How to enumerate the potential layer combinations for the candidate vertices? In the following, we address these two issues in detail.

4.1 Candidate Vertices Identification

It is costly to compute the exact SynCore for a graph. An alternative is to find candidate vertices and then refine them to the final results. To this end, we introduce the concept of Quasi-SynCore.

Definition 4.1. (Quasi-SynCore). Given a multilayer graph $G = (V, E, L)$, an integer k , and a support threshold $1 \leq s \leq |L|$, the Quasi-SynCore of G on layer set L , denoted by QSC_s^k , is a maximal vertex set $H \subseteq V$ such that for each vertex $v \in H$:

- (i) there are at least s layers $L' \subseteq L$ satisfying $\deg_{L'}^H(v) \geq k$ on each layer $l \in L'$;
- (ii) in the projected graph G_P of G , $\deg_P^H(v) \geq k + 1$.

The Quasi-SynCore does not require specific layers to meet the k -core structure. Instead, each vertex may satisfy the degree constraints on different s layers. For example, in Figure 1, given $k = 2$ and $s = 2$, the Quasi-SynCore is $\{v_3, v_4, v_5, v_6, v_7, v_8, v_9\}$. The Quasi-SynCore and SynCore have the following relationship.

LEMMA 4.1. Given integers k and $s \in [1, |L|]$, and layers $L' \subseteq L$ with $|L'| = s$. Then, $SC_{L'}^k \subseteq QSC_s^k$.

According to Lemma 4.1, QSC_s^k is a superset of $SC_{L'}^k$. Hence, we can take the vertices of QSC_s^k as candidate vertices. For example, given $k = 2$, $s = 2$, and $L' = \{1, 2\}$ for multilayer graph in Figure 1. $SC_{\{1,2\}}^2 = \{v_3, v_4, v_5, v_6, v_7\}$, it is a subset of $QSC_2^2 = \{v_3, v_4, v_5, v_6, v_7, v_8, v_9\}$.

Algorithm 1: Quasi-SynCore Computation

Input: A multilayer graph $G(V, E, L)$, projected graph G_P , integers k and s
Output: the Quasi-SynCore

```

1 foreach  $v \in V$  do
2   compute  $\deg_P(v) - 1$ ;
3    $Top-s(v) \leftarrow$  the  $s$ -th largest degree among all layers in  $L$ ;
4    $syn-deg(u) \leftarrow \min(Top-s(v), \deg_P(v) - 1)$ ;
5 while  $V \neq \emptyset$  do
6    $v \leftarrow$  vertex with minimum  $syn-deg(u)$  in  $V$ ;
7   if  $syn-deg(u) \geq k$  then
8     break;
9    $V \leftarrow V \setminus v$ ;  $V' \leftarrow \emptyset$ ; //  $V'$  stores affected vertices
10  foreach  $(v, u, l) \in E$  and  $syn-deg(u) \geq k$  do
11    if  $\deg_l(u) = syn-deg(u)$  then
12       $V' \leftarrow V' \cup u$ ;
13     $\deg_l(u) \leftarrow \deg_l(u) - 1$ ;
14  foreach  $(v, u) \in E_P$  and  $syn-deg(u) \geq k$  do
15    if  $\deg_P(u) - 1 = syn-deg(u)$  then
16       $V' \leftarrow V' \cup u$ ;
17     $\deg_P(u) \leftarrow \deg_P(u) - 1$ ;
18  foreach  $u \in V'$  do
19    recompute  $Top-s(u)$ ;
20    update  $syn-deg(u)$ ;
21 return  $V$ ;
```

Next, we introduce how to compute the Quasi-SynCore efficiently. First, we introduce the concepts of degree vector, $Top-s$ degree, and synergetic degree. Specifically, the degree vector of a vertex v on a set of layers L' , denoted by $\mathbf{deg}_{L'}(v) = [\deg_{l_1}(v), \deg_{l_2}(v), \dots, \deg_{l_{|L'|}}(v)]$, consists of the degrees of v on all layers in L' . The $Top-s$ degree of $\mathbf{deg}_{L'}(v)$, denoted by $Top-s(v)$, is the s -th largest degree in the degree vector $\mathbf{deg}_{L'}(v)$. The synergetic degree of v , denoted by $syn-deg(v)$, is the minimum of the $Top-s$ degree and the degree in the projected graph minus 1, i.e., $syn-deg(v) = \min(Top-s(v), \deg_P(v) - 1)$. For example, the degree vector of v_4 in Figure 1 is $\mathbf{deg}_L(v_4) = [3, 3, 2]$, and its degree in the projected graph is 5. So the synergetic degree of v_4 when $s = 2$ is $syn-deg(v_4) = 3$.

LEMMA 4.2. Given integers k and s , for a vertex $v \in V$, if $syn-deg(v) < k$, $v \notin QSC_s^k$.

According to Lemma 4.2, if the synergetic degree of a vertex v is less than k , v is not included in the Quasi-SynCore. Thus, v can be safely deleted, which leads to an update of synergetic degrees for v 's neighbors. However, recomputing the synergetic degrees for all v 's neighbors is costly due to the $Top-s$ degrees calculation. To tackle this issue, we propose the following lemma to identify v 's neighbors whose synergetic degrees do not need updating.

LEMMA 4.3. Assume a vertex $v \in V$ is deleted from a multilayer graph G , and u is a neighbor of v . If $syn-deg(u)$ satisfies (i) $syn-deg(u) \neq \deg_P(u) - 1$, and (ii) $\forall l \in L$ with $(v, u, l) \in E$, $syn-deg(u) \neq \deg_l(u)$, $syn-deg(u)$ does not need to be updated.

Lemma 4.3 reduces the number of neighbors whose synergetic degree needs to be recomputed. Only the neighbor u whose degree on a particular layer equals $syn-deg(u)$ or whose degree in the projected graph equals $syn-deg(u) + 1$ could be affected.

Based on the above discussion, we propose an algorithm for Quasi-SynCore computation. Algorithm 1 shows the pseudo-code. Specifically, firstly, Algorithm 1 computes the degree in the projected graph, $Top-s$ degree, and synergetic degree for each vertex

(lines 3-4). Then, Algorithm 1 iteratively deletes the vertex with the minimal synergetic degree (lines 5-21). After a vertex is deleted (lines 6 and 9), Algorithm 1 updates the synergetic degree of the deleted vertex's neighbors. In particular, for the v 's neighbor u , Algorithm 1 updates u 's degree on each layer (lines 10-13) and the projected graph (lines 14-17). Suppose $deg_l(u) = syn-deg(u)$ or $deg_p(u) - 1 = syn-deg(u)$, u will be added to the set of affected vertices (lines 11-12, 15-16). Then, the $Top-s$ degree and synergetic degree of each affected vertex is updated (lines 18-20). Finally, the Quasi-SynCore is returned (line 21).

Complexity Analysis. The time complexity of of Algorithm 1 is $O(|L| \cdot (|E| + |V|))$. Algorithm 1 takes $O(|L|)$ time to get the s -largest value in a degree vector using a divide and conquer method. Hence, computing the $Top-s$ degree for all vertices takes $O(|L| \cdot |V|)$ time. During the computation process, each vertex is removed at most once, which takes $O(|V|)$ time. In addition, the update of $Top-s$ degrees takes $O(|L| \cdot |E|)$ time. Therefore, the total time complexity is $O(|L| \cdot (|E| + |V|))$.

4.2 Potential Layer Combination Enumeration

In the previous subsection, we introduce Quasi-SynCore as the candidate for the final result. In this subsection, we present how to enumerate potential layer combinations for a given Quasi-SynCore. Given a multilayer graph $G = (V, E, L)$, let QSC_s^k be the Quasi-SynCore of G , the potential layer combination enumeration aims to identify the layer combinations that may contain the final result according to QSC_s^k .

According to Definition 4.1, the degree of a vertex $v \in QSC_s^k$ is not less than k on at least s layers of L . We call these layers the matched layers of v , denoted by $ML(v)$, i.e., $ML(v) = \{l \mid l \in L, deg_l(v) \geq k\}$. A potential layer combination L' should be a subset of L , making Quasi-SynCore on L' closer to a SynCore than QSC_s^k . Since the final result must contain query vertex set Q , we enumerate the layer combination based on the matched layers of $q \in Q$ as follows.

Enumeration Rules. We consider two cases.

- (1) If $|\bigcap_{q \in Q} ML(q)| < |L|$, one layer combination $L' = \bigcap_{q \in Q} ML(q)$ should be enumerated.
- (2) If $|\bigcap_{q \in Q} ML(q)| = |L|$, $\forall l \in L$, all layer combinations with $L' = L - l$ should be enumerated.

The $\bigcap_{q \in Q} ML(q)$ is the intersection of matched layers of all vertices in the query vertex set. On each layer of the intersection, the degrees of all query vertices are greater than or equal to k . This intersection represents a set of layers that may contain the final results. If $|\bigcap_{q \in Q} ML(q)| < |L|$, this intersection is an ideal layer combination that is a proper subset of L . Thus, only one layer combination L' needs to be enumerated, i.e., $L' = \bigcap_{q \in Q} ML(q)$. Otherwise, we need to enumerate more than one layer combination according to L . Each enumerated layer combination L' is obtained by removing one layer from L .

For the potential layer combination enumeration, one important issue is how to terminate the enumeration. To this end, we provide the termination rules.

Termination Rules. The layer combination enumeration can be terminated if one of the following conditions is satisfied.

Algorithm 2: Progressive Search Algorithm (PSA)

Input: a multilayer Graph $G = (V, E, L)$, $k \geq 0$, $s \in [1, |L|]$, query vertices $Q \subseteq V$
Output: maximum connected SynCore containing Q

```

1  $H \leftarrow \emptyset$ ; construct projected graph  $G_P$  of  $G$ ;
2  $QSC_s^k \leftarrow \text{Quasi-SynCore\_Computation}((V, E, L), G_P, k, s)$ ;
3  $QSC_s^k.PL \leftarrow L$ ;
4 add  $QSC_s^k$  to  $T$ ; //  $T$  stores Quasi-SynCores
5 while  $T \neq \emptyset$  do
6    $QSC_s^k \leftarrow$  pop the Quasi-SynCore with the largest size from  $T$ ;
7   if  $|QSC_s^k| < |H|$  then
8     break;
9    $L_{QSC} \leftarrow QSC_s^k.PL$ ;
10  compute the matched layers  $ML(v)$  for each  $v \in QSC_s^k$ ;
11  if  $\bigcap_{v \in QSC_s^k} ML(v) = L_{QSC}$  then // Termination Rule 1
12     $H' \leftarrow$  the connected component of  $QSC_s^k$  containing  $Q$ ;
13    if  $|H'| > |H|$  then
14       $H \leftarrow H'$ ;
15    continue;
16  // Enumeration Rules
17   $PL \leftarrow \emptyset$ ; //  $PL$  stores potential layer combinations
18  if  $|\bigcap_{q \in Q} ML(q)| < |L_{QSC}|$  then
19     $PL \leftarrow \bigcap_{q \in Q} ML(q)$ ;
20  else
21     $PL \leftarrow$  all subsets of  $L_{QSC}$  with  $|L_{QSC}| - 1$  layers;
22  foreach  $L' \in PL$  do
23    // Termination Rules 2 and 3
24    if  $|L'| < s$  or  $L'$  has been enumerated then
25      continue;
26     $V' \leftarrow$  all vertices of  $QSC_s^k$ ;
27    foreach  $v \in V'$  do
28      if  $|ML(v) \cap L'| < s$  then
29         $V' \leftarrow V' \setminus v$ ;
30     $QSC_s^k \leftarrow \text{Quasi-SynCore\_Computation}((V', E, L'), G_P, k, s)$ ;
31     $QSC_s^k.PL \leftarrow L'$ ;
32    // Termination Rule 4
33    if  $QSC_s^k \neq \emptyset$  and  $Q \subseteq QSC_s^k$  then
34      add  $QSC_s^k$  to  $T$ ;
35 return  $H$ ;

```

- (1) If $\bigcap_{v \in QSC_s^k} ML(v) = L$, enumeration according to L can be stopped.
- (2) If $|L'| < s$, L' can be pruned.
- (3) If L' has been enumerated before, then L' can be pruned.
- (4) If the corresponding Quasi-SynCore of L' is empty or Q is not included in the Quasi-SynCore, then L' can be pruned.

We illustrate the termination rules one by one. (1) If all vertices in QSC_s^k have the same matched layers, QSC_s^k is a SynCore on L . Therefore, there is no need to enumerate any new layer combination L' . Note that $|L|$ may be larger than s . (2) If the cardinality of L' is less than s , the Quasi-SynCore corresponding to L' cannot be a SynCore. Thus, the layer combination L' does not need to be enumerated. (3) Each layer combination is enumerated at most once. The enumeration process will not generate duplicate layer combinations. (4) If the Quasi-SynCore corresponding to L' is empty or does not contain Q , it cannot be the final result of SynCS. Hence, L' should not be enumerated.

4.3 Progressive Search Algorithm

Based on the above discussions, we propose the algorithm PSA. Given a multilayer graph G , PSA firstly computes the Quasi-SynCore for G . Then, PSA enumerates the potential layer combinations

according to the *Enumeration Rules*. For each layer combination L' , PSA computes the Quasi-SynCore' w.r.t., L' . Afterwards, PSA iteratively enumerates the potential layer combinations for the Quasi-SynCore' and computes the new Quasi-SynCore'' until the termination rules are satisfied. Note that the Quasi-SynCore' is not necessarily computed from scratch. We only need to take the Quasi-SynCore on the corresponding layer combination L' as a multilayer graph to compute the Quasi-SynCore'.

The pseudo-code of PSA is outlined in Algorithm 2. First, PSA performs some initializations (line 1); computes the Quasi-SynCore of the graph G (line 2); set the layer combination of Quasi-SynCore to L (line 3); and adds it to a heap T (line 4). Subsequently, PSA iteratively enumerates potential layer combinations and computes the corresponding Quasi-SynCores (lines 5-31). In each round, PSA checks the Quasi-SynCore QSC_s^k with the largest size (line 6). If the size of QSC_s^k is smaller than the currently found maximum SynCore, QSC_s^k can not contain the solution (lines 7-8). Otherwise, PSA computes the matched layers for all vertices in QSC_s^k based on the (line 9). If all vertices QSC_s^k share the same matched layers, the QSC_s^k is a SynCore. Hence, PSA gets the connected component of QSC_s^k containing the query vertices Q to check whether it is the final result (lines 11-15). Otherwise, PSA enumerates the layer combinations according to Enumeration Rules (lines 16-20), in which the invalid layer combinations are pruned according to Termination Rules (2) and (3) (lines 21-22). For each remaining potential layer combination L' , PSA filters invalid vertices in QSC_s^k (lines 25-27), and employs Algorithm 1 to compute the new Quasi-SynCore $QSC_s'^k$ on the layer L' (line 28). If $QSC_s'^k$ is not empty or Q is included in $QSC_s'^k$, $QSC_s'^k$ will be added to T for further processing (lines 30-31). Finally, PSA returns SynCS (line 32).

Complexity Analysis. Let N be the total number of Quasi-SynCores computed by PSA, and N' be the number of Quasi-SynCores that do not generate new potential layer combinations based on termination rules. The time complexity of PSA is $O(N \cdot |L| \cdot |V| + N' \cdot |L| \cdot (|E| + |V|))$. PSA primarily involves enumeration and the computation for Quasi-SynCores. For enumeration, PSA computes matched layers for each Quasi-SynCore, taking $O(|L| \cdot |V|)$ time. Thus, the total time complexity of enumeration is $O(N \cdot |L| \cdot |V|)$. The computation for each Quasi-SynCore is based on an existing Quasi-SynCore, not from scratch. Therefore, the computation for all Quasi-SynCores takes $O(N' \cdot |L| \cdot (|E| + |V|))$ time. Therefore, the total complexity of PSA is $O(N \cdot |L| \cdot |V| + N' \cdot |L| \cdot (|E| + |V|))$.

5 TRIE-BASED SEARCH ALGORITHM

The progressive search algorithm improves the efficiency by reducing the enumeration of layer combinations. For a given multilayer graph, SynCores on different layers can be pre-computed. In light of this, we propose a novel index called Dominant Layers-based Trie (DLT) to compactly store all SynCores for efficient synergetic community search.

5.1 DLT Structure

Let k_{max} be the maximum k value of all non-empty SynCores in the multilayer graph. Totally, there are $k_{max} \cdot \binom{L}{s}$ SynCores. Hence, it is essential to design a compact index to reduce the index storage.

Firstly, we introduce some features of the SynCore, which are useful for index design.

PROPERTY 1. (Uniqueness). Given a multilayer graph $G = (V, E, L)$, an integer k , and a layer set $L' \subseteq L$, $SC_{L'}^k$ is unique.

PROPERTY 2. (Hierarchy). Given a multilayer graph $G = (V, E, L)$, an integer k , and two layer combinations L' and L'' with $L'' \subseteq L' \subseteq L$. Then, $SC_{L'}^{k+1} \subseteq SC_{L'}^k$ and $SC_{L'}^k \subseteq SC_{L''}^k$.

Based on these two properties, different SynCores have inclusion relations for different layers and values of k . Inspired by this, we propose the concept of dominant layers.

Definition 5.1. (Dominant Layers). Given a multilayer graph $G = (V, E, L)$, a vertex $v \in V$, and an integer $k \geq 0$. Layers $L' \subseteq L$ are dominant layers of v if the following two conditions are satisfied. (i) $v \in SC_{L'}^k$; (ii) $\nexists L'' \subseteq L$ such that $L' \subset L''$ and $v \in SC_{L''}^k$.

For example, in Figure 1, $v_4 \in SC_{\{1\}}^2$, $v_4 \in SC_{\{1,2\}}^2$, and $v_4 \notin SC_{\{1,2,3\}}^2$. Hence, $\{1, 2\}$ are the dominant layers of v_4 . For a fixed k value, a vertex v may belong to the $SC_{L'}^k$ for different sets of dominant layers. We use $DL_k(v) = \{L_1, L_2, \dots, L_n\}$ to denote all sets of dominant layers of v w.r.t., k . According to Property 2, if $v \in SC_{L'}^k$, $\forall L''' \subset L'$, $v \in SC_{L'''}^k$. Therefore, based on $DL_k(v)$, we can find all SC_L^k containing v .

In light of this, we present the Dominant Layers-based Trie (DLT) to organize all sets of dominant layers into a trie. Each DLT corresponds to a fixed k . By default, we assume that the dominant layers in a set are in ascending order of their IDs. The structure of DLT is shown in Figure 3. The root node of DLT is an empty node. The non-root node D of DLT consists of two parts: (i) $D.Layer$: a layer $l \in L$, and (ii) $D.Vertex$: a dominant vertex set DV_i of the dominant layers represented by D . Each node D_i represents a layer combination consisting of layers from the root node to D_i . We use $L(D_i)$ to denote the layer combination represented by node D_i . The dominant vertex set DV_i of D_i consists of vertices whose sets of dominant layers contains $L(D_i)$, i.e., $DV_i = \{v \in V \mid L(D_i) \in DL_k(v)\}$. Each vertex v may have more than one set of dominant layers, and it can appear in multiple DV_i s. To quickly locate the DV_i s containing the query vertices, a vertex map $VM_k(v)$ is employed to store which DV_i s a vertex belongs to.

Example 2. We take Figure 1 as an example. Let $k = 2$. The set of dominant layers of each vertex is shown in Figure 4(a). Totally, there are two sets of dominant layers, i.e. $\{v_1, v_2\}$ and $\{v_3\}$. The corresponding DLT is depicted in Figure 4(b).

Complexity Analysis. Let θ be the average number of sets of dominant layers for a vertex when k is specified. The space complexity of all DLTs is $O(\theta \cdot |E| \cdot |L|)$. For a vertex $v \in V$, the maximum possible k corresponding to the SynCore to which it belongs is $\sum_{l \in L} deg_l(v)$. Therefore, the total number of sets of dominant layers for all vertices is bounded by $O(\sum_{v \in V} (\theta \cdot \sum_{l \in L} deg_l(v))) = O(\theta \cdot |E|)$. The space cost of DLTs mainly consists of two parts: (i) the structure of the trie and (ii) the dominant vertex set of trie nodes. For the first part, its complexity is the same as the total number of DLT nodes, which is bounded by $O(\theta \cdot |E| \cdot |L|)$. For the second part, its complexity is the total number of sets of dominant layers for all vertices, which is $O(\theta \cdot |E|)$. Thus, the space complexity of all DLTs is $O(\theta \cdot |E| \cdot |L|)$.

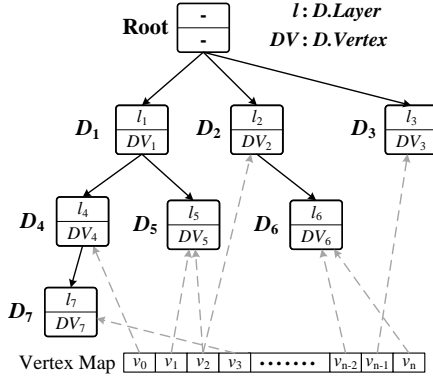


Figure 3: The structure of DLT

5.2 DLT Construction

In this subsection, we present DLT construction method. The basic idea of DLT construction is to firstly compute all SynCores for a given multilayer graph. Then, we compute all sets of the dominant layers, based on which DLT is built. First, we introduce SynCore decomposition to compute all SynCores.

SynCore Decomposition.

We formally define the SynCore decomposition as follows.

Definition 5.2. (SynCoreness). Given a multilayer graph $G = (V, E, L)$, a vertex $v \in V$, and a set of layers $L' \subseteq L$, the SynCoreness of v , denoted by $C_{L'}(v)$, is the largest k such that v is in $SC_{L'}^k$. Formally, $C_{L'}(v) = \max_{v \in SC_{L'}^k} k$.

Definition 5.3. (SynCore Decomposition). Given a multilayer graph $G = (V, E, L)$, and a set of layers $L' \subseteq L$, the SynCore decomposition computes the SynCoreness for $\forall v \in V$ and $\forall L' \subseteq L$.

According to Definition 5.3, a straightforward method for SynCore decomposition is to compute SynCore for all possible L' 's directly, which is costly. To efficiently perform SynCore decomposition, we exploit the local property of SynCore.

Lemma 5.1. Given a multilayer graph $G = (V, E, L)$, a vertex $v \in V$, and a set of layers $L' \subseteq L$, $C_{L'}(v) = k$ if and only if k is the largest value satisfying:

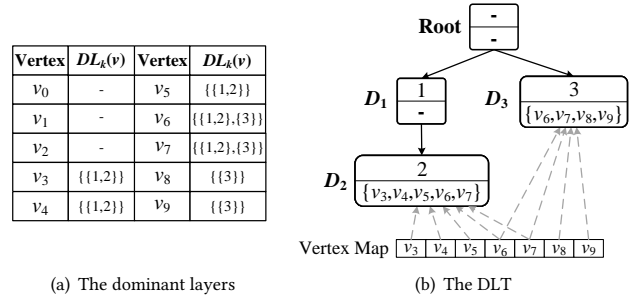
(i) On each layer $l \in L'$, there are k neighbors $u \in N_l(v)$ such that $C_{L'}(u) \geq k$.

(ii) In the projected graph, there are $k + 1$ neighbors $up \in N_p(v)$ such that $C_{L'}(up) \geq k$.

According to Lemma 5.1, $C_{L'}(v)$ can be computed according to the SynCoreness of v 's neighbors. Specifically, $C_{L'}(v) = \max k$ s.t. $\forall l \in L', |\{u \in N_l(v) \mid C_{L'}(u) \geq k\}| \geq k$, and $|\{up \in N_p(v) \mid C_{L'}(up) \geq k\}| \geq k + 1$. Nevertheless, we are unaware of the vertices' SynCoreness. An alternative is to set $C_{L'}(v)$ with an upper bound, denoted by $\bar{C}_{L'}(v)$. And then, we iteratively update the $\bar{C}_{L'}(v)$ until it converges to $C_{L'}(v)$. Here, we need to address the following issues.

(1) How to set the upper bound $\bar{C}_{L'}(v)$ for v ? (2) When to update the $\bar{C}_{L'}(v)$? (3) How to update the $\bar{C}_{L'}(v)$?

How to set the upper bound $\bar{C}_{L'}(v)$ for v ? For a vertex $v \in V$, the SynCoreness satisfies $C_{L'}(v) \leq \deg_p(v)$. In addition, based on the hierarchy property (i.e., Property 2), for $L'' \subset L'$, $SC_{L'}^k$ is a subset of $SC_{L''}^k$. Hence, $C_{L'}(v) \leq C_{L''}(v)$. Therefore, $\bar{C}_{L'}(v)$ can be set as follows. If $\exists L'' \subset L'$, $\bar{C}_{L'}(v)$ can initially be set to $\min_{L'' \subset L'} C_{L''}(v)$. Otherwise, $\bar{C}_{L'}(v) = \deg_p(v)$.



(a) The dominant layers

(b) The DLT

Figure 4: Examples of dominant layers and DLT

When to update the $\bar{C}_{L'}(v)$? First, we give some useful definitions.

For a layer $l \in L'$, we use $sup_l(v)$ to denote the the number of v 's neighbors on layer l , whose upper bound of SynCoreness is no less than $\bar{C}_{L'}(v)$, i.e. $sup_l(v) = |\{u \in N_l(v) \mid \bar{C}_{L'}(u) \geq \bar{C}_{L'}(v)\}|$. Likewise, $sup_p(v)$ is defined as the number of v 's neighbors in the projected graph, whose upper bound of SynCoreness is no less than $\bar{C}_{L'}(v)$, i.e. $sup_p(v) = |\{u \in N_p(v) \mid \bar{C}_{L'}(u) \geq \bar{C}_{L'}(v)\}|$. $\bar{C}_{L'}(v)$ needs to be updated when it satisfies the following lemma.

Lemma 5.2. Given a multilayer graph $G = (V, E, L)$, a vertex $v \in V$, and layers $L' \subseteq L$, if $\exists l \in L'$ such that $sup_l(v) < \bar{C}_{L'}(v)$, or $sup_p(v) < \bar{C}_{L'}(v) + 1$, $\bar{C}_{L'}(v)$ needs to be updated.

How to update the $\bar{C}_{L'}(v)$? When v satisfies Lemma 5.2, $\bar{C}_{L'}(v)$ is updated as follows. (1) For each layer $l \in L'$, we compute k_l , which is the maximum k satisfying that v has at least k neighbors $u \in N_l(v)$ such that $\bar{C}_{L'}(u) \geq k$. Formally, $k_l = \max k$ s.t. $|\{u \in N_l(v) \mid \bar{C}_{L'}(u) \geq k\}| \geq k$. (2) In the projected graph, we compute k_p . Specifically, $k_p = \max k$ s.t. $|\{u \in N_p(v) \mid \bar{C}_{L'}(u) \geq k\}| \geq k + 1$. After computing k_l 's and k_p , $\bar{C}_{L'}(v)$ is updated to $\min_{l \in L'} \{k_l, k_p\}$.

In what follows, we give the pseudocode of SynCore decomposition, which is shown in Algorithm 3. The algorithm enumerates all layer combinations with the cardinality from 1 to $|L|$ (lines 2-3). For each enumerated layer combination L' , if L' only contains one layer, the upper bound $\bar{C}_{L'}(v)$ is set to the degree in the projected graph (line 6). Otherwise, $\bar{C}_{L'}(v)$ is set to the minimum SynCoreness of v among all previously enumerated layer combinations $L'' \subset L'$ (line 8). Then, Algorithm 3 computes the SynCorenesses of vertices for L' employing the function *Compute_SynCoreness* (line 9).

The function *Compute_SynCoreness* is outlined in lines 11-31 of Algorithm 3. It firstly computes $sup_l(v)$ and $sup_p(v)$ for each vertex (lines 11-14), and then identifies the vertex v , whose $\bar{C}_{L'}(v)$ needs to be updated, according to Lemma 5.2 (line 15). Next, $\bar{C}_{L'}(v)$ is updated (lines 16-21). Subsequently, $sup_l(v)$ and $sup_p(v)$ of v , and $sup_l(u)$ and $sup_p(u)$ of v 's neighbor u are updated according to the new $\bar{C}_{L'}(v)$ (lines 22-30). If there does not exist a vertex v , whose $\bar{C}_{L'}(v)$ needs to be updated, the function terminates.

Dominant layers Computation and DLTs Construction

When completing the SynCore decomposition, we should compute all sets of the dominate layers for every vertex. Specifically, consider a layer combination $L' \subseteq L$, an integer $k \geq 0$, and a vertex $v \in V$. If $C_{L'}(v) \geq k$ and there is no $L'' \subset L'$ such that the SynCoreness of v on L'' is greater than or equal to k , L' is a set of dominant layers of v . Therefore, all sets of dominant layers of v for a given k are $DL_k(v) = \{L' \subseteq L \mid C_{L'}(v) \geq k \wedge \nexists L'' \subseteq L \text{ such that } L' \subset L'' \text{ and } C_{L''}(v) \geq k\}$.

Algorithm 3: SynCore Decomposition

Input: multilayer graph G
Output: the SynCorenesses of all vertices

```

1 construct projected graph  $G_P$  of  $G$ ;
2 foreach  $s = 1$  to  $|L|$  do
3   foreach layers  $L' \subseteq L$  and  $|L'| = s$  do
4     foreach  $v \in V$  do
5       if  $s = 1$  then
6          $\bar{C}_{L'}(v) \leftarrow \text{deg}_P(v)$ ;
7       else
8          $\bar{C}_{L'}(v) \leftarrow \min_{L'' \subset L'} C_{L''}(v)$ ;
9      $C_{L'} \leftarrow \text{Compute\_SynCoreness}(G, G_P, L', \bar{C}_{L'})$ 
10 return  $C_{L'}$  for all  $L' \subseteq L$ 

Procedure Compute_SynCoreness( $G, G_P, L', \bar{C}_{L'}$ )
11 foreach  $v \in V$  do
12   foreach  $l \in L'$  do
13      $\text{sup}_l(v) \leftarrow |\{u \in N_l(v) \mid \bar{C}_{L'}(u) \geq \bar{C}_{L'}(v)\}|$ ;
14    $\text{sup}_P(v) \leftarrow |\{u \in N_P(v) \mid \bar{C}_{L'}(u) \geq \bar{C}_{L'}(v)\}|$ ;
15 while  $\exists v \in V, l \in L'$  such that  $\text{sup}_l(v) < \bar{C}_{L'}(v)$  or
     $\text{sup}_P(v) \leq \bar{C}_{L'}(v) + 1$  do
16    $ub \leftarrow \bar{C}_{L'}(v)$ ;
17   foreach  $l \in L'$  do
18      $k_l(v) \leftarrow \max k \text{ s.t. } |\{u \in N_l(v) \mid \bar{C}_{L'}(u) \geq k\}| \geq k$ ;
19      $\bar{C}_{L'}(v) \leftarrow \min(k_l(v), \bar{C}_{L'}(v))$ ;
20    $k_P(v) \leftarrow \max k \text{ s.t. } |\{u \in N_P(v) \mid \bar{C}_{L'}(u) \geq k\}| \geq k + 1$ ;
21    $\bar{C}_{L'}(v) \leftarrow \min(k_P(v), \bar{C}_{L'}(v))$ ;
22   foreach  $l \in L'$  do
23      $\text{sup}_l(v) \leftarrow |\{u \in N_l(v) \mid \bar{C}_{L'}(u) \geq \bar{C}_{L'}(v)\}|$ ;
24     foreach  $u \in N_l(v)$  do
25       if  $\bar{C}_{L'}(u) \leq ub$  and  $\bar{C}_{L'}(u) > \bar{C}_{L'}(v)$  then
26          $\text{sup}_l(u) \leftarrow \text{sup}_l(u) - 1$ ;
27    $\text{sup}_P(v) \leftarrow |\{u \in N_P(v) \mid \bar{C}_{L'}(u) \geq \bar{C}_{L'}(v)\}|$ ;
28   foreach  $u \in N_P(v)$  do
29     if  $\bar{C}_{L'}(u) \leq ub$  and  $\bar{C}_{L'}(u) > \bar{C}_{L'}(v)$  then
30        $\text{sup}_P(u) \leftarrow \text{sup}_P(u) - 1$ ;
31 return  $\bar{C}_{L'}$ ;

```

After computing all sets of dominant layers, the DLT for k is then constructed by accessing all sets of dominant layers of all vertices. We assume that the layers in dominant layers are in ascending order of their ID. Hence, each set of dominant layers can be treated as a string and we can build a trie for all sets of dominant layers. One point should be highlighted is that, when building trie, each node of trie is augmented with the dominant vertex set DV_i .

Based on the above discussions, the procedure for DLT Construction is outlined in Algorithm 4. The algorithm first employs the SynCore decomposition algorithm to obtain all SynCorenesses for all vertices (line 1). Once the decomposition is complete, the algorithm enumerates k from 0 to its maximum value to build the DLTs. For each k , a trie node is initialized as the root for a DLT (lines 4-5). Then, all sets of dominant layers for each vertex v are computed (line 7). For each set of dominant layers of v , its layers are traversed, building the DLT by visiting from the root node (lines 8-19). Consider a layer number l and a visited DLT node D . If there is a child node of D' with layer number l , the child node will be visited (lines 11-12). Otherwise, a new DLT node with l will be created (lines 14-15). If l is the last number of the set of dominant

Algorithm 4: DLT Construction Algorithm

Input: multilayer graph G
Output: DLT

```

1 All SynCorenesses  $\leftarrow \text{SynCore\_Decomposition}(G)$ ;
2  $DLT \leftarrow \emptyset$ ;
3 foreach  $k = 0$  to  $k_{\max}$  do
4   initialize a root trie node  $D_{\text{root}}$ ;
5    $DLT[k] \leftarrow D_{\text{root}}$ ;
6   foreach  $v \in V$  do
7      $DL_k(v) = \{L' \subseteq L \mid C_{L'}(v) \geq k \wedge \nexists L'' \subseteq L \text{ such that } L' \subset L'' \text{ and } C_{L''}(v) \geq k\}$ ;
8     foreach  $L' \in DL_k(v)$  do
9        $D \leftarrow DLT[k]$ ; //  $D$  is a root node
10      foreach  $l \in L'$  do
11        if  $\exists D' \in D.\text{child}$  such that  $D'.\text{Layer} = l$  then
12           $D \leftarrow D'$ ;
13        else
14          create a new node  $D'$ ;  $D'.\text{Layer} = l$ ;
15           $D.\text{child.add}(D')$ ;  $D \leftarrow D'$ ;
16        if  $l$  is the last number of  $L'$  then
17           $D.\text{Vertex.add}(v)$ ;
18           $VM_k(v).\text{add}(D)$ ;
19 return  $DLT$ ;

```

layers, v is added to the dominant vertex set of the node, and the node is added to the vertex map of v (lines 16-18). Finally, DLTs for all possible k are returned.

Complexity Analysis. Let θ be the average number of dominant layers for each vertex when k is specified, and U_{\max} be the maximum upper bound of SynCoreness for any vertex. The time complexity of Algorithm 4 is $O(2^{|L|} \cdot (|L| \cdot |V| + U_{\max} \cdot |E|) + \theta \cdot |E| \cdot |L|)$. The time cost of Algorithm 4 consists of two parts: (i) SynCore decomposition and (ii) DLT building. For the decomposition phase on layers $L' \subseteq L$, it takes $O(|L| \cdot |V|)$ time to set the upper bound of SynCoreness and $O(U_{\max} \cdot |E|)$ time to perform the decomposition. With $2^{|L|} - 1$ combinations, the total time is $O(2^{|L|} \cdot (|L| \cdot |V| + U_{\max} \cdot |E|))$. For the DLT building phase, each set of dominant layers of vertices is accessed for a specific k , taking $O(\theta \cdot |E| \cdot |L|)$ time. Therefore, The time complexity of Algorithm 4 is $O(2^{|L|} \cdot (|L| \cdot |V| + U_{\max} \cdot |E|) + \theta \cdot |E| \cdot |L|)$.

5.3 DLT-based Search Algorithm

Based on the DLT index, we develop an efficient DLT-based search algorithm (DSA) to handle SynCS. The main idea of DSA is as follows. It firstly finds all dominant layer sets $DL_k(q)$ for each query vertex $q \in Q$, and uses dominant layer sets $DL_k(q)$ to enumerate all layer combinations that contain s layers for q . If a layer combination L' is enumerated for all query vertices, Q is contained in $SC_{L'}^k$. All such layer combinations constitute candidate layer combinations. Next, for each candidate layer combination L' , DSA traverses the DLT to find all vertices of $SC_{L'}^k$ via matching. Finally, $SC_{L'}^k$ with the maximum size is returned.

The pseudocode of DSA is shown in Algorithm 5. First, DSA obtains all sets of dominant layers for each query vertex q by utilizing the vertex map $VM_k(q)$ (line 5). For each set of dominant layers, different combinations of s layers are stored in $tempSetL$ (line 7). The $setL$ stores the intersection of layer combinations for s layers of all query vertices (line 8). Then, for each combination $L' \in setL$, a stack S is used to perform DFS on the DLT. DSA pushes

Algorithm 5: DLT-based Search Algorithm (DSA)

Input: multilayer graph G , projected graph G_P , $k \geq 0$, $s \in [1, |L|]$, query vertices Q , DLTs
Output: the SynCore H

```

1  $H \leftarrow \emptyset$ ;  $setL \leftarrow$  all combinations of  $s$  layers;
2 foreach  $q \in Q$  do
3    $tempSetL \leftarrow \emptyset$ ;
4   foreach  $D \in VM_k(q)$  do
5      $L' \leftarrow$  layer combination represented by  $D$ ;
6     foreach  $L'' \subseteq L'$  and  $|L''| = s$  do
7        $tempSetL.add(L'')$ ;
8    $setL \leftarrow tempSetL \cap setL$ ;
9 foreach  $L' \in setL$  do
10   $S.push((DLT[k], 0))$  //  $S$  is a stack
11   $H' \leftarrow \emptyset$ ;
12  while  $S \neq \emptyset$  do
13     $(D, i) \leftarrow$  pop the top element from  $S$ ;
14    if  $D.Layer = L'[i]$  then
15      if  $i < |L'| - 1$  then
16         $i \leftarrow i + 1$ ;
17      else
18        foreach  $D'$  in the subtree of  $D$  do
19           $add D'.Vertex$  to  $H'$ ;
20        continue;
21      foreach  $D' \in D.Child$  do
22        if  $D'.Layer \leq L'[i]$  then
23           $S.push((D', i))$ ;
24   $H' \leftarrow$  connected component of  $H'$  that contains  $Q$ ;
25  if  $|H'| \geq |H|$  then
26     $H \leftarrow H'$ ;
27 return  $H$ ;

```

the root node into the stack with the matched number $i = 0$ (line 10). For each element popped from the stack, i.e., DLT node D and the matched number i , DSA matches the node and pushes potential child nodes into S according to the *Matching Mechanism* (lines 14-23). When DSA gets the $SC_{L'}^k$, it searches the connected component that contains the query vertex set (line 24). The maximum connected component is the result of SynCS (line 27).

Example 3. In the DLT of Figure 4(b), given $k = 2$, $s = 2$, and $Q = \{v_5\}$, since v_5 is in the dominant vertex set of node D_2 , the possible layer combination is $\{1, 2\}$. Then, DSA starts from the root, node D_1 and node D_2 are matched sequentially, and $\{v_3, v_4, v_5, v_6, v_7\}$ are added to the result. Node D_3 cannot be matched. The final result is $\{v_3, v_4, v_5, v_6, v_7\}$.

Complexity Analysis. Let \mathcal{H} be the number of vertices of the final result, and λ be the number of candidate layer combinations of the query vertex set. The time complexity of Algorithm 5 is $O(\lambda \cdot (\mathcal{H} + |L| \cdot \log(|L|)))$. There are $O(\lambda \cdot |L|)$ DLT nodes to be accessed. Choosing child nodes for each DLT node takes $O(\log |L|)$ time. So traversing the DLT takes $O(\lambda \cdot |L| \cdot \log(|L|))$ time. The time cost of aggregating results is proportional to the total number of vertices in the result, i.e., $O(\mathcal{H})$. Therefore, the total time complexity is $O(\lambda \cdot (\mathcal{H} + |L| \cdot \log(|L|)))$.

5.4 DLT Maintenance

In this subsection, we discuss DLT maintenance. After some vertices or edges are inserted or deleted from the multilayer graph, the SynCoreness of some vertices may change. Let V^* denote the vertices whose SynCoreness has changed. Let $C_{L'}^*(v)$ denote the new SynCoreness of $v \in V^*$ on layers $L' \subseteq L$.

Table 1: Statistics of networks

$\overline{|DL(v)|}$: the average number of dominant layer sets for a vertex; θ : the average number of dominant layer sets per vertex for a given k ; K: 10^3 ; M: 10^6 ; B: 10^9

Dataset	Abbr.	V	E	L	$\overline{ DL(v) }$	θ
Slashdot [20]	SD	51K	139K	6	1.3	0.33
Homo [52]	HM	18K	153K	7	6.1	0.64
SacchCere [52]	SC	6.5K	247K	7	29.0	1.22
DBLP [19]	DB	512K	1.0M	10	1.4	0.44
Obama [52]	OB	2.2M	3.8M	3	0.5	0.15
YEAST [52]	YE	4.5K	8.5M	4	1635.2	0.99
Higgs [52]	HI	456K	13M	4	27.5	0.89
StackOverflow [44]	SO	2.6M	64.5M	9	8.5	0.69
Wiki [30]	WK	6.9M	129M	10	5.9	0.66
MAG [22]	MG	53M	1.1B	8	7.2	0.78

For each affected vertex, we first compute its new sets of dominant layers when k is specified, denoted as $DL_k^*(v)$. Specifically, $DL_k^*(v) = \{L' \subseteq L \mid C_{L'}^*(v) \geq k \wedge \nexists L'' \supset L' \text{ s.t. } C_{L''}^*(v) \geq k\}$. Once we obtain the new sets of dominant layers for a vertex, the collection of newly added sets of dominant layers is $DL_k^+(v) = DL_k^*(v) \setminus DL_k(v)$, and the collection of deleted sets of dominant layers is $DL_k^-(v) = DL_k(v) \setminus DL_k^*(v)$.

For each set of newly added dominant layers L^+ , let $V(L^+)$ denote the vertices whose newly added dominant layers set contains L^+ , i.e., $V(L^+) = \{v \in V \mid L^+ \in DL_k^+(v)\}$. Then, L^+ is treated as a string, and inserted into the DLT. If a node corresponding to the prefix of L^+ does not exist, a new DLT node is created. For the DLT node whose represented prefix matches L^+ , we add $V(L^+)$ to the dominant vertex set of that node. For each set of deleted dominant layers L^- , let $V(L^-)$ denote the vertices whose deleted dominant layers set contains L^- , i.e., $V(L^-) = \{v \in V \mid L^- \in DL_k^-(v)\}$. For the node whose represented prefix matches L^- , $V(L^-)$ is deleted from its dominant vertex set. If a leaf node has an empty dominant vertex set, it is deleted.

6 EXPERIMENTS

This section evaluates the performance of the index structure and algorithms we propose. The experiments use [ten](#) real-world multilayer graphs, details of which are summarized in Table 3. All algorithms were implemented in C++ and compiled by GCC 9.3.0 with -O3 optimization. All experiments were conducted on a machine running on Ubuntu server 20.04.2 LTS version with an Intel(R) Core(TM) i9-10900K CPU @ 3.70GHz and 128GB memory. In each experiment, we randomly generate 1,000 sets of query vertices, and report the average results. [The experimental results for all datasets are available in our technical report \[41\].](#)

6.1 Effectiveness Evaluation

First, we evaluate the effectiveness of our proposed SynCore model.

Exp-1: Community Quality Comparison of Different Models. We assess the quality of communities retrieved by different models under their optimal parameter settings.

Competitors. We compare SynCore with [seven](#) cohesive subgraph models for multilayer graphs, i.e., d -CC [36, 53], FirmCore [20], FocusCore [50], CrossCore[46], k -core [19], and FirmTruss [4].

Table 2: Community quality comparison for different models under the optimal parameter settings
(Metrics: ①: *D-Avg*, ②: *D-Min*, ③: *D-P*, ④: *GCC-Avg*, ⑤: *GCC-Min*, ⑥: *GCC-P*)

Datasets	HM						DB						HI						WK						MG					
Metrics	①	②	③	④	⑤	⑥	①	②	③	④	⑤	⑥	①	②	③	④	⑤	⑥	①	②	③	④	⑤	⑥	①	②	③	④	⑤	⑥
SynCore	0.78	0.73	0.88	0.83	0.81	0.91	0.66	0.60	0.72	0.84	0.73	0.85	0.50	0.43	0.80	0.65	0.55	0.74	0.53	0.40	0.79	0.86	0.71	0.93	0.64	0.45	0.76	0.51	0.40	0.97
<i>d</i> -CC	0.49	0.48	0.67	0.69	0.68	0.81	0.42	0.42	0.61	0.70	0.69	0.71	0.41	0.30	0.71	0.42	0.36	0.55	0.37	0.34	0.73	0.72	0.63	0.79	0.44	0.38	0.60	0.39	0.36	0.79
FirmCore	0.40	0.07	0.54	0.53	0.08	0.63	0.28	0.02	0.45	0.40	0.09	0.54	0.24	0.03	0.47	0.25	0.03	0.33	0.28	0.02	0.57	0.47	0.04	0.69	0.32	0.05	0.35	0.31	0.03	0.63
FocusCore	0.69	0.62	0.75	0.80	0.73	0.83	0.53	0.52	0.64	0.72	0.72	0.79	0.46	0.37	0.81	0.46	0.41	0.55	-	-	-	-	-	-	-	-	-	-	-	-
CrossCore	0.49	0.48	0.67	0.69	0.68	0.81	0.42	0.42	0.61	0.70	0.69	0.71	0.41	0.30	0.71	0.42	0.36	0.55	0.37	0.34	0.73	0.72	0.63	0.79	-	-	-	-	-	-
<i>k</i> -core	0.55	0.48	0.69	0.74	0.72	0.82	0.43	0.43	0.62	0.75	0.72	0.78	0.42	0.31	0.73	0.43	0.36	0.59	-	-	-	-	-	-	-	-	-	-	-	-
(<i>k</i> +1)-core	0.31	0.05	0.42	0.33	0.06	0.49	0.21	0.01	0.31	0.25	0.07	0.33	0.16	0.02	0.29	0.18	0.02	0.20	0.22	0.02	0.45	0.28	0.03	0.50	0.20	0.03	0.34	0.20	0.02	0.47
FirmTruss	0.52	0.09	0.64	0.64	0.16	0.73	0.47	0.06	0.52	0.61	0.20	0.88	0.41	0.06	0.70	0.36	0.14	0.66	-	-	-	-	-	-	-	-	-	-	-	-

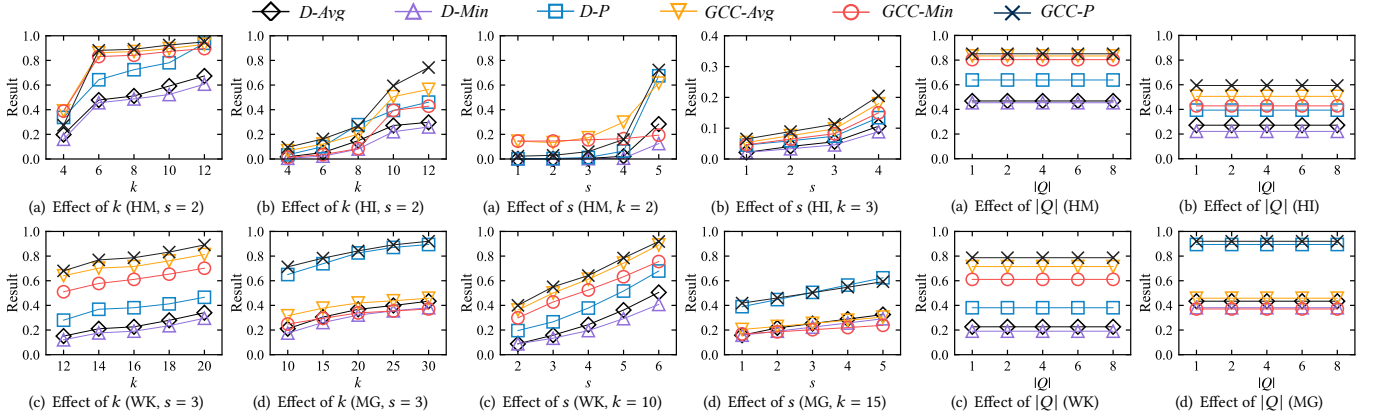


Figure 5: Effect of k on community quality

Figure 6: Effect of s on community quality

Figure 7: Effect of $|Q|$ on community quality

We also compare the community returned by $(k+1)$ -core in the projected graph.

Metrics. To evaluate the quality of the discovered communities, we employ two types of metrics: the *density* ($\frac{2 \cdot |E|}{|V| \cdot (|V|-1)}$) [8] and the *global clustering coefficient* ($\frac{3 \cdot |\Delta|}{|triplet|}$) [40]. Let H be the returned community; $D_l[H]$ and $GCC_l[H]$ (rep. $D_P[H]$ and $GCC_P[H]$) are the density and global clustering coefficient of H on layer l (rep. projected graph), respectively; and L_c is the set of layers that satisfy the degree constraints of cohesive subgraph models.

(1) The density-based metrics include *average density* ($D-Avg$), *minimum density* ($D-Min$), and *density in the projected graph* ($D-P$) of H , which are defined as follows.

$$D-Avg = \frac{\sum_{l \in L_c} D_l[H]}{|L_c|}, \quad D-Min = \min_{l \in L_c} D_l[H], \quad D-P = D_P[H]$$

(2) The global clustering coefficient-based metrics consist of *average global clustering coefficient* ($GCC-Avg$), *minimum global clustering coefficient* ($GCC-Min$), and *global clustering coefficient in the projected graph* ($GCC-P$). Specifically,

$$GCC-Avg = \frac{\sum_{l \in L_c} GCC_l[H]}{|L_c|},$$

$$GCC-Min = \min_{l \in L_c} GCC_l[H], \quad GCC-P = GCC_P[H]$$

Results. The community quality of all models under their optimal parameter settings on five datasets are shown in Table 2. Note that "-" represents that evaluating the quality of all parameter combinations for the model could not be completed within 24 hours. Overall, SynCore shows superior quality compared to other models. This is because SynCore considers both local and global cohesiveness,

enabling it to identify highly cohesive communities. Other models like *d*-CC, CrossCore, and *k*-core only consider cohesiveness on partial layers, resulting in lower densities and clustering coefficients compared to SynCore. As for FirmCore and FirmTruss, they do not require dense structures across layers, leading to lower-quality communities. FocusCore, which simply combines *d*-CC and FirmCore, does not enhance community quality. The $(k+1)$ -core in the projected graph performs the worst, showing that the quality of SynCore is not solely reliant on projected graph constraints. These results demonstrate the effectiveness of SynCore's design.

Exp-2: Effect of Parameters on Community Quality. In this set of experiments, we investigate the effects of different parameters on SynCore, including k , s , and $|Q|$. Figures 5 to 7 presents the results. **Effect of k** (Figure 5): As k increases, all metrics consistently improve, indicating that higher k values lead to more cohesive subgraphs. This is because increasing k results in more neighbors, thereby enhancing community cohesiveness. **Effect of s** (Figure 6): In general, increasing s improves the community quality. This is because larger s requires more layers to meet the degree constraint, resulting in denser community structures. **Effect of $|Q|$** (Figure 7): We can observe that when $|Q|$ varies, the qualities of communities almost keep the same. It is because the query vertex sets of different sizes belong to the same community.

Exp-3: Case Study on DBLP. In this experiment, we conduct a case study on DBLP [12]. We collected papers from VLDB, SIGMOD, ICDE, and KDD to construct a four-layer graph. Each vertex represents an author, and each layer corresponds to a conference. An edge exists between two authors within a layer if they have coauthored a paper in that conference. The core models used in this study are SynCore, *d*-CC, FocusCore, CrossCore, FirmCore,

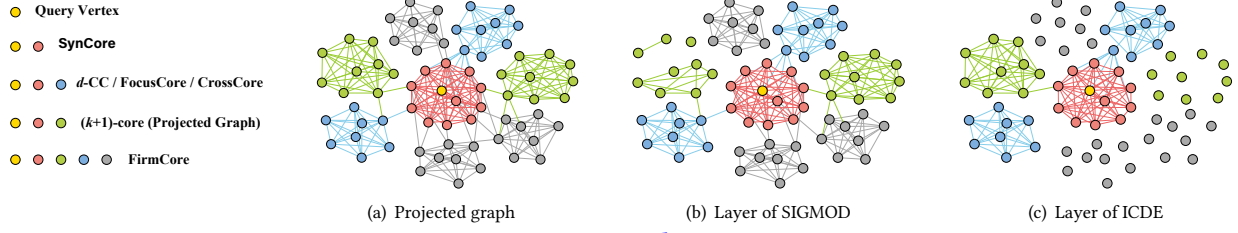


Figure 8: Case study on DBLP

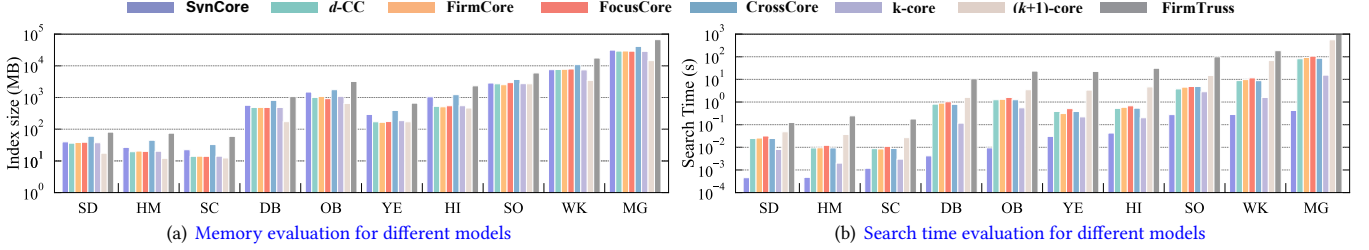


Figure 9: Efficiency comparison for different models

and $(k + 1)$ -core in the projected graph. To conduct community search, we set the query vertex Q = Samuel Madden; $k = k_{max} = 7$ to ensure the returned community is non-empty; and $s = 2$. For d -CC and FocusCore, we specify SIGMOD and ICDE as the layers of interest. For FirmCore, we set $\lambda = 2$. Figure 8 shows the connected subgraphs returned by these models. All subgraphs contain the query vertex, which is highlighted in yellow. The community identified by SynCore (red and yellow vertices) stands out as the most cohesive, evidently constituting a close network of academic collaborators. The collaborators exhibit strong cohesiveness not only within the SIGMOD and ICDE, but also form a tighter network across the four data-related conferences. For the communities identified by other models, some authors who do not closely collaborate with the query vertex are included in the result. For example, in d -CC / FocusCore / CrossCore (blue, red, and yellow vertices), the set of blue vertices in the bottom left has only one edge connecting to the main red cluster, which should not be included in the result.

6.2 Efficiency Evaluation

We evaluate the efficiency of our proposed algorithms, including the *DLT-based Search Algorithm* (DSA), the *Progressive Search Algorithm* (PSA), and the *Basic Method* (BM). The evaluation includes memory usage and search time. Besides, we test parameters including k , s , $|Q|$, $|L|$, and $|V|$. Each experiment varies one parameter while keeping the others at default values. k and s are set by the datasets, $|Q|$ defaults to 1, and $|L|$ and $|V|$ use original dataset values. We report running time, using INF for any that exceed 10^4 seconds.

Exp-4: Efficiency Comparison of Different Models. In this experiment, we evaluate the *Peak Memory Usage* and *Average Search Time* for different models. The results across ten datasets are presented in Figure 9. Figure 9(a) shows that the memory usage of SynCore is slightly higher than that of d -CC, FirmCore, and FocusCore. This is because enumerating layer combinations requires additional memory. However, SynCore consumes less memory compared to CrossCore and FirmTruss. CrossCore needs to explore more layer combinations than SynCore, while FirmTruss’s complex structure results in naturally higher memory usage. Figure 9(b) demonstrates that the search time of SynCore is faster by several

orders of magnitude compared to other models. This is largely due to the acceleration provided by the DLT.

Exp-5: Effect of Parameters on Search Time. In this set of experiments, we investigate the effects of different parameters on search time, including k , s , $|Q|$, and $|L|$. Results are shown in Figures 10 to 13, respectively. Overall, DSA consistently outperforms PSA and BM by 1-5 orders of magnitude while PSA is better than BM. This is because DSA leverages the DLT index to avoid multiple graph traversals. In contrast, BM must enumerate all possible layer combinations. PSA improves upon BM by pruning invalid combinations. However, it still needs traversals the original graph to compute SynCore, which makes PSA slower than DSA. **Effect of k** (Figure 10): As k increases, DSA becomes faster because a larger k results in a smaller SynCore, reducing the number of DLT nodes it needs to traverse. PSA and BM are not significantly affected by k as k does not impact the number of layer combinations. **Effect of s** (Figure 11): Increasing s reduces DSA’s search time by decreasing the size of SynCore. For BM, increasing s results in more layer combinations, leading to longer search times. PSA maintains stable performance by pruning combinations effectively. **Effect of $|Q|$** (Figure 12): As $|Q|$ increases, DSA and PSA show slight decreases in search time due to fewer layer combinations. BM’s search time remains constant since it must compute SynCore for all combinations regardless of $|Q|$. **Effect of $|L|$** (Figure 13): Increasing $|L|$ deteriorates the performance of all algorithms due to an expanded search space from more layer combinations.

Exp-6: Scalability The scalability of the three algorithms is shown in Figure 14. In this experiment, we randomly sampled vertices from the original graph to generate graphs with varying sizes. As expected, the performance of all algorithms declines as the graph size increases, since larger graphs lead to larger communities. However, DSA and PSA consistently outperform BM by several orders of magnitude, highlighting their superior efficiency. On the MG dataset, the proposed DSA and PSA methods demonstrate high efficiency, while the baseline BM fails to finish within 10^4 seconds. The remarkable efficiency of DSA and PSA can be attributed to their highly effective pruning capabilities.

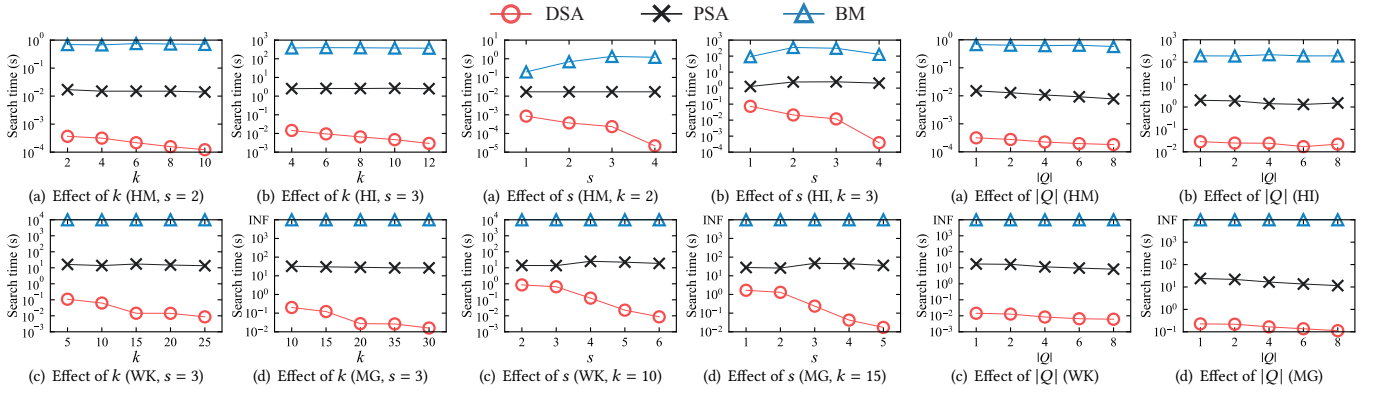


Figure 10: Effect of k on search time

Figure 11: Effect of s on search time

Figure 12: Effect of $|Q|$ on search time

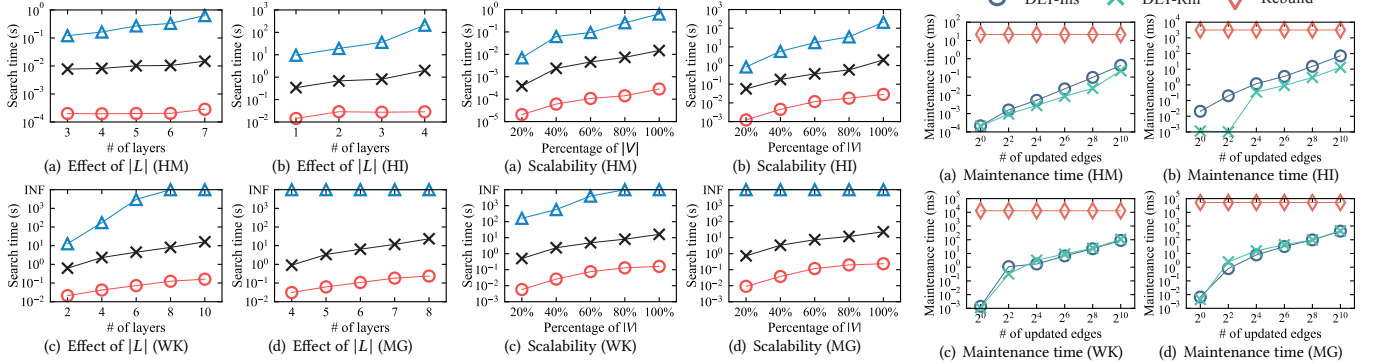


Figure 13: Effect of $|L|$ on search time

Figure 14: Scalability

Figure 15: DLT maintenance evaluation

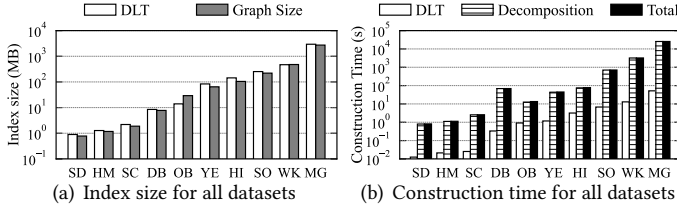


Figure 16: DLT construction evaluation

6.3 Index Evaluation

In this section, we examine the performance of DLT, focusing on both its construction and maintenance.

Exp-7: DLT Construction. In this experiment, we test the DLT size and construction time on all datasets. The results are shown in Figure 16. Figure 16(a) shows that the index size of DLT is comparable to the graph size in all datasets. For example, the sizes of DLT and the original graph of MG are 2944 MB and 2729 MB, respectively. The compactness of DLT benefits from the design of dominant layers, which allows DLT to store only a small subset of layer combinations. The construction time of DLT is shown in Figure 16(b), where *Decomposition* denotes the SynCore decomposition time, *DLT* denotes the time of dominant layers computation and DLT construction, and *Total* is the sum of *Decomposition* and *DLT*. We can observe that the majority of the time is spent on SynCore decomposition. Building the DLT itself takes only a small fraction of the total time. On MG dataset, *Decomposition* and *DLT* take 25,477s and 51s, respectively, with DLT Construction accounting for 0.2% of the total time. The reason behind this is that *Decomposition* needs to compute SynCores for all possible layer combinations, which takes a lot of time. Notably, even on large dataset MG, *Decomposition* still shows good performance. This is because *Decomposition* employs

the reuse technique, which avoids recomputing SynCore for each layer combination from scratch.

Exp-8: DLT Maintenance. Finally, we evaluate the performance of DLT maintenance by randomly inserting and removing different numbers of edges, ranging from 2^0 to 2^{10} . Results are shown in Figure 15. *DLT-Ins* and *DLT-Rm* denote the maintenance algorithms for edge insertion and removal, respectively. *Rebuild* denotes to build the index from scratch whenever the multilayer graph updates. We have two key observations. First, both *DLT-Ins* and *DLT-Rm* are more efficient than *Rebuild*. Second, the performance of both *DLT-Ins* and *DLT-Rm* degenerates as the number of inserted/removed edges increases. This is because, as more edges are updated, more SynCores are affected, resulting in more sets of dominant layers being changed. Therefore, *DLT-Ins* and *DLT-Rm* require more time to maintain the DLT.

7 CONCLUSION

In this paper, we study the problem of synergetic community search over large multilayer graphs. First, we devise a new cohesive model called synergetic core (SynCore). Based on SynCore, we formally define the synergetic core community search problem. To solve the problem efficiently, we propose a progressive search algorithm that substantially reduces the search space. To enhance the search efficiency further, we design a novel index called dominant layers-based trie (DLT). We develop a DLT-based search algorithm by traversing DLT to return the community. Extensive experimental results on large real-world datasets validate the effectiveness and efficiency of our proposed model and algorithms. In the future, we would like to investigate the truss-based cohesive subgraph model for multilayer graphs to handle the synergetic community search.

REFERENCES

- [1] Esra Akbas and Peixiang Zhao. 2017. Truss-based community search: A truss-equivalence based indexing approach. *Proceedings of the VLDB Endowment* 10, 11 (2017), 1298–1309.
- [2] Asim Ansari, Oded Koenigsberg, and Florian Stahl. 2011. Modeling multiple relationships in social networks. *Journal of Marketing Research* 48, 4 (2011), 713–728.
- [3] Nicola Barbieri, Francesco Bonchi, Edoardo Galimberti, and Francesco Gullo. 2015. Efficient and effective community search. *Data mining and knowledge discovery* 29 (2015), 1406–1433.
- [4] Ali Behrouz, Farnoosh Hashemi, and Laks VS Lakshmanan. 2022. FirmTruss community search in multilayer networks. *Proceedings of the VLDB Endowment* 16, 3 (2022), 505–518.
- [5] Lijun Chang, Xuemin Lin, Lu Qin, Jeffrey Xu Yu, and Wenjie Zhang. 2015. Index-based optimal algorithms for computing steiner components with maximum connectivity. In *Proceedings of the 2015 ACM SIGMOD International Conference on Management of Data*. 459–474.
- [6] Lu Chen, Chengfei Liu, Rui Zhou, Jiajie Xu, Jeffrey Xu Yu, and Jianxin Li. 2020. Finding effective geo-social group for impromptu activities with diverse demands. In *Proceedings of the 26th ACM SIGKDD International Conference on Knowledge Discovery & Data Mining*. 698–708.
- [7] Chaitali Choudhary, Inder Singh, and Manoj Kumar. 2023. Community detection algorithms for recommendation systems: Techniques and metrics. *Computing* 105, 2 (2023), 417–453.
- [8] Thomas F Coleman and Jorge J Moré. 1983. Estimation of sparse jacobian matrices and graph coloring blems. *SIAM journal on Numerical Analysis* 20, 1 (1983), 187–209.
- [9] Andrea Fronzetti Colladon and Elisa Remondi. 2017. Using social network analysis to prevent money laundering. *Expert Systems with Applications* 67 (2017), 49–58.
- [10] Wanyun Cui, Yanghua Xiao, Haixun Wang, Yiqi Lu, and Wei Wang. 2013. Online search of overlapping communities. In *Proceedings of the 2013 ACM SIGMOD international conference on Management of data*. 277–288.
- [11] Wanyun Cui, Yanghua Xiao, Haixun Wang, and Wei Wang. 2014. Local search of communities in large graphs. In *Proceedings of the 2014 ACM SIGMOD international conference on Management of data*. 991–1002.
- [12] DBLP. 2024. <https://dblp.uni-trier.de/xml/>
- [13] Mark E Dickison, Matteo Magnani, and Luca Rossi. 2016. *Multilayer social networks*. Cambridge University Press.
- [14] Yixiang Fang, Reynold Cheng, Xiaodong Li, Siqiang Luo, and Jiafeng Hu. 2017. Effective community search over large spatial graphs. *Proceedings of the VLDB Endowment* 10, 6 (2017), 709–720.
- [15] Yixiang Fang, Reynold Cheng, Siqiang Luo, and Jiafeng Hu. 2016. Effective community search for large attributed graphs. *Proceedings of the VLDB Endowment* 9, 12 (2016).
- [16] Yixiang Fang, Xin Huang, Lu Qin, Ying Zhang, Wenjie Zhang, Reynold Cheng, and Xuemin Lin. 2020. A survey of community search over big graphs. *The VLDB Journal* 29 (2020), 353–392.
- [17] Yixiang Fang, Zhongran Wang, Reynold Cheng, Hongzhi Wang, and Jiafeng Hu. 2018. Effective and efficient community search over large directed graphs. *IEEE Transactions on Knowledge and Data Engineering* 31, 11 (2018), 2093–2107.
- [18] Yixiang Fang, Yixing Yang, Wenjie Zhang, Xuemin Lin, and Xin Cao. 2020. Effective and efficient community search over large heterogeneous information networks. *Proceedings of the VLDB Endowment* 13, 6 (2020), 854–867.
- [19] Edoardo Galimberti, Francesco Bonchi, and Francesco Gullo. 2017. Core decomposition and densest subgraph in multilayer networks. In *Proceedings of the 2017 ACM Conference on Information and Knowledge Management*. 1807–1816.
- [20] Farnoosh Hashemi, Ali Behrouz, and Laks VS Lakshmanan. 2022. Firmcore decomposition of multilayer networks. In *Proceedings of the ACM Web Conference 2022*. 1589–1600.
- [21] Haiyan Hu, Xifeng Yan, Yu Huang, Jiawei Han, and Xianghong Jasmine Zhou. 2005. Mining coherent dense subgraphs across massive biological networks for functional discovery. *Bioinformatics* 21, suppl_1 (2005), i213–i221.
- [22] Weihua Hu, Matthias Fey, Hongyu Ren, Maho Nakata, Yuxiao Dong, and Jure Leskovec. 2021. Ogb-lsc: A large-scale challenge for machine learning on graphs. *arXiv preprint arXiv:2103.09430* (2021).
- [23] Hongxuan Huang, Qingyuan Linghu, Fan Zhang, Dian Ouyang, and Shiyu Yang. 2021. Truss decomposition on multilayer graphs. In *2021 IEEE International Conference on Big Data (Big Data)*. 5912–5915.
- [24] Xin Huang, Hong Cheng, Lu Qin, Wentao Tian, and Jeffrey Xu Yu. 2014. Querying k-truss community in large and dynamic graphs. In *Proceedings of the 2014 ACM SIGMOD international conference on Management of data*. 1311–1322.
- [25] Xin Huang, Laks VS Lakshmanan, and Jianliang Xu. 2019. *Community search over big graphs*. Morgan & Claypool Publishers.
- [26] Xin Huang, Laks VS Lakshmanan, Jeffrey Xu Yu, and Hong Cheng. 2015. Approximate closest community search in networks. *Proceedings of the VLDB Endowment* 9, 4 (2015), 276–287.
- [27] Xun Jian, Yue Wang, and Lei Chen. 2020. Effective and efficient relational community detection and search in large dynamic heterogeneous information networks. *Proceedings of the VLDB Endowment* 13, 10 (2020), 1723–1736.
- [28] Daxin Jiang and Jian Pei. 2009. Mining frequent cross-graph quasi-cliques. *ACM Transactions on Knowledge Discovery from Data (TKDD)* 2, 4 (2009), 1–42.
- [29] Yuli Jiang, Yu Rong, Hong Cheng, Xin Huang, Kangfei Zhao, and Junzhou Huang. 2022. Query driven-graph neural networks for community search: From non-attributed, attributed, to interactive attributed. *Proceedings of the VLDB Endowment* 15, 6 (2022), 1243–1255.
- [30] KONECT. 2013. <http://konect.uni-koblenz.de/networks>
- [31] Ling Li, Siqiang Luo, Yuhai Zhao, Caihua Shan, Zhengkui Wang, and Lu Qin. 2023. COCLEP: Contrastive learning-based semi-supervised community search. In *2023 IEEE 39th International Conference on Data Engineering (ICDE)*. 2483–2495.
- [32] Rong-Hua Li, Jiao Su, Lu Qin, Jeffrey Xu Yu, and Qiangqiang Dai. 2018. Persistent community search in temporal networks. In *2018 IEEE 34th International Conference on Data Engineering (ICDE)*. 797–808.
- [33] Yuqi Li, Tao Meng, Zhixiong He, Haiyan Liu, and Keqin Li. 2024. A biased edge enhancement method for truss-based community search. *Frontiers of Computer Science* 18, 3 (2024), 183610.
- [34] Kar Wai Lim and Wray Buntine. 2016. Bibliographic analysis on research publications using authors, categorical labels and the citation network. *Machine Learning* 103, 2 (2016), 185–213.
- [35] Longlong Lin, Pingpeng Yuan, Rong-Hua Li, Chunxue Zhu, Hongchao Qin, Hai Jin, and Tao Jia. 2024. QTCS: Efficient query-centered temporal community search. *Proceedings of the VLDB Endowment* 17, 6 (2024), 1187–1199.
- [36] Boge Liu, Fan Zhang, Chen Zhang, Wenjie Zhang, and Xuemin Lin. 2019. Corecube: Core decomposition in multilayer graphs. In *Web Information Systems Engineering—WISE 2019: 20th International Conference, Hong Kong, China, January 19–22, 2020, Proceedings* 20. Springer, 694–710.
- [37] Dandan Liu and Zhaonian Zou. 2023. gCore: Exploring cross-Layer cohesiveness in multi-layer graphs. *Proceedings of the VLDB Endowment* 16, 11 (2023), 3201–3213.
- [38] Qing Liu, Minjun Zhao, Xin Huang, Jianliang Xu, and Yunjun Gao. 2020. Truss-based community search over large directed graphs. In *Proceedings of the 2020 ACM SIGMOD International Conference on Management of Data*. 2183–2197.
- [39] Qing Liu, Yifan Zhu, Minjun Zhao, Xin Huang, Jianliang Xu, and Yunjun Gao. 2020. VAC: Vertex-centric attributed community search. In *2020 IEEE 36th International Conference on Data Engineering (ICDE)*. 937–948.
- [40] R Duncan Luce and Albert D Perry. 1949. A method of matrix analysis of group structure. *Psychometrika* 14, 2 (1949), 95–116.
- [41] Chengyang Luo, Qing Liu, Yunjun Gao, and Jianliang Xu. 2024. Synergetic Community Search over Large Multilayer Graphs. <https://github.com/ZJU-DAILY/SynCore/blob/main/SynCore-VLDB25-FullVersion.pdf>
- [42] Fragkiskos D Malliaros, Christos Giatsidis, Apostolos N Papadopoulos, and Michalis Vazirgiannis. 2020. The core decomposition of networks: Theory, algorithms and applications. *The VLDB Journal* 29, 1 (2020), 61–92.
- [43] David W Matula and Leland L Beck. 1983. Smallest-last ordering and clustering and graph coloring algorithms. *Journal of the ACM (JACM)* 30, 3 (1983), 417–427.
- [44] SNAP. 2014. <http://snap.stanford.edu/data>
- [45] Mauro Sozio and Aristides Gionis. 2010. The community-search problem and how to plan a successful cocktail party. In *Proceedings of the 16th ACM SIGKDD international conference on Knowledge discovery and data mining*. 939–948.
- [46] Longxu Sun, Xin Huang, Zheng Wu, and Jianliang Xu. 2024. Efficient Cross-layer Community Search in Large Multilayer Graphs. In *2024 IEEE 40th International Conference on Data Engineering (ICDE)*. 2959–2971.
- [47] Jianwei Wang, Kai Wang, Xuemin Lin, Wenjie Zhang, and Ying Zhang. 2024. Efficient unsupervised community search with pre-trained graph transformer. *Proceedings of the VLDB Endowment* 17, 9 (2024), 2227–2240.
- [48] Jianwei Wang, Kai Wang, Xuemin Lin, Wenjie Zhang, and Ying Zhang. 2024. Neural attributed community search at billion scale. *Proceedings of the ACM on Management of Data* 1, 4 (2024), 1–25.
- [49] Kai Wang, Wenjie Zhang, Xuemin Lin, Ying Zhang, Lu Qin, and Yuting Zhang. 2021. Efficient and effective community search on large-scale bipartite graphs. In *2021 IEEE 37th International Conference on Data Engineering (ICDE)*. 85–96.
- [50] Run-An Wang, Dandan Liu, and Zhaonian Zou. 2024. FocusCore decomposition of multilayer graphs. In *2024 IEEE 40th International Conference on Data Engineering (ICDE)*. 2792–2804.
- [51] Yue Wang, Xun Jian, Zhenhua Yang, and Jia Li. 2017. Query optimal k-plex based community in graphs. *Data Science and Engineering* 2 (2017), 257–273.
- [52] Manlio De Domenico’s website. 2017. <https://manliodedomenico.com/data.php>
- [53] Rong Zhu, Zhaonian Zou, and Jianzhong Li. 2018. Diversified coherent core search on multi-layer graphs. In *2018 IEEE 34th International Conference on Data Engineering (ICDE)*. 701–712.

APPENDIX

A PROOFS OF LEMMAS AND THEOREMS

A.1 Proof of Lemma 4.1

LEMMA 4.1 Given integers k and $s \in [1, |L|]$, and layers $L' \subseteq L$ with $|L'| = s$. Then, $SC_{L'}^k \subseteq QSC_s^k$.

PROOF. For the $SC_{L'}^k$, it is a k -core on each layer $l \in L'$. Thus, the degrees of any vertex in $SC_{L'}^k$ are no less than k on each layers in L' , meeting condition (i) in Definition 4.1. In the projected graph, the degree of each vertex in $SC_{L'}^k$ is greater than k , satisfying condition (ii) in Definition 4.1. Hence, $SC_{L'}^k \subseteq QSC_s^k$. \square

A.2 Proof of Lemma 4.2

LEMMA 4.2 Given integers k and s , for a vertex $v \in V$, if $\text{syn-deg}(v) < k$, $v \notin QSC_s^k$.

PROOF. If $\text{syn-deg}(v) < k$, it means $\text{Top-s}(v) < k$ or $\text{deg}_p(v) - 1 < k$. If $\text{Top-s}(v) < k$, there does not exist s layers, on which v has k neighbors. If $\text{deg}_p(v) - 1 < k$, it does not satisfy the degree constraint on the projected graph. Therefore, $v \notin QSC_s^k$. \square

A.3 Proof of Lemma 4.3

LEMMA 4.3 Assume a vertex $v \in V$ is deleted from a multilayer graph G , and u is a neighbor of v . If $\text{syn-deg}(u)$ satisfies (i) $\text{syn-deg}(u) \neq \text{deg}_p(u) - 1$, and (ii) $\forall l \in L$ with $(v, u, l) \in E$, $\text{syn-deg}(u) \neq \text{deg}_l(u)$, $\text{syn-deg}(u)$ does not need to be updated.

PROOF. If $\text{syn-deg}(u) = \text{deg}_p(u) - 1$, the deletion of v will decrease u 's degree in the projected graph, resulting in a change of $\text{syn-deg}(u)$. Hence, the necessary condition for $\text{syn-deg}(u)$ not to be updated is $\text{syn-deg}(u) \neq \text{deg}_p(u) - 1$. In other words, $\text{syn-deg}(u) = \text{Top-s}(u)$.

If $\forall l \in L$ with $(v, u, l) \in E$, $\text{syn-deg}(u) \neq \text{deg}_l(u)$, $\text{Top-s}(u) = \text{deg}_{l'}(u)$, where $(v, u, l') \notin E$. After deleting v , $\text{Top-s}(u) = \text{deg}_{l'}(u)$ and $\text{Top-s}(u) \leq \text{deg}_p(u) - 2$. Therefore, $\text{syn-deg}(u) = \text{Top-s}(u)$. \square

A.4 Proof of Lemma 5.1

LEMMA 5.1 Given a multilayer graph $G = (V, E, L)$, a vertex $v \in V$, and a set of layers $L' \subseteq L$, $C_{L'}(v) = k$ if and only if k is the largest value satisfying:

- (i) On each layer $l \in L'$, there are k neighbors $u \in N_l(v)$ such that $C_{L'}(u) \geq k$.
- (ii) In the projected graph, there are $k + 1$ neighbors $u_p \in N_p(v)$ such that $C_{L'}(u_p) \geq k$.

PROOF. (1) *Necessity*. If $C_{L'}(v) = k$, then $v \in SC_{L'}^k$. On each layer $l \in L'$, there exists k neighbors belonging to $SC_{L'}^k$. In the projected graph, there exists $k + 1$ neighbors included in $SC_{L'}^k$. Suppose k is not the largest value that satisfies the conditions, then $v \in SC_{L'}^{k+1}$. This contradicts to $C_{L'}(v) = k$.

(2) *Sufficiency*. According to conditions (i) and (ii), v and its neighbors form a k -core on each layer $l \in L$, and they form a $(k + 1)$ -core in the projected graph. Therefore, $v \in SC_{L'}^k$. Since k is the largest value that satisfies the conditions, the SynCoreness of v is k . \square

A.5 Proof of Lemma 5.2

LEMMA 5.2 Given a multilayer graph $G = (V, E, L)$, a vertex $v \in V$, and layers $L' \subset L$, if $\exists l \in L'$ such that $\text{supp}_l(v) < \bar{C}_{L'}(v)$, or $\text{supp}(v) < \bar{C}_{L'}(v) + 1$, $\bar{C}_{L'}(v)$ needs to be updated.

PROOF. If $\exists l \in L'$ such that $\text{supp}_l(v) < \bar{C}_{L'}(v)$, v and its neighbors cannot form a $\bar{C}_{L'}(v)$ -core on layer l . Similarly, if $\text{supp}(v) < \bar{C}_{L'}(v) + 1$, v and its neighbors cannot form a $(\bar{C}_{L'}(v) + 1)$ -core in the projected graph. Therefore, the $\bar{C}_{L'}(v)$ should be updated. \square

B DATASETS

Table 3: Statistics of networks
 $\overline{|DL(v)|}$: the average number of dominant layer sets for a vertex; θ : the average number of dominant layer sets per vertex for a given k ; K: 10^3 ; M: 10^6 ; B: 10^9

Dataset	Abbr.	V	E	L	$\overline{ DL(v) }$	θ
Slashdot [20]	SD	51K	139K	6	1.3	0.33
Homo [52]	HM	18K	153K	7	6.1	0.64
SacchCere [52]	SC	6.5K	247K	7	29.0	1.22
DBLP [19]	DB	512K	1.0M	10	1.4	0.44
Obama [52]	OB	2.2M	3.8M	3	0.5	0.15
YEAST [52]	YE	4.5K	8.5M	4	1635.2	0.99
Higgs [52]	HI	456K	13M	4	27.5	0.89
StackOverflow [44]	SO	2.6M	64.5M	9	8.5	0.69
Wiki [30]	WK	6.9M	129M	10	5.9	0.66
MAG [22]	M	53M	1.1B	8	7.2	0.78

We provide an introduction to the datasets used in this study. The Slashdot dataset represents social interactions within the Slashdot network. It consists of six layers, with each layer representing interactions that occurred within a specific month. The Homo dataset [52] is a genetic interactions dataset, with each layer corresponding to a specific type of interaction, such as direct interaction, physical association, suppressive or additive genetic interactions defined by inequality, colocalization, and synthetic genetic interactions. The SacchCere dataset [20], another genetic interactions dataset, shares the same layer definitions as the Homo dataset. The DBLP dataset [19] represents a co-authorship network, where each layer corresponds to a data mining topic, and an edge exists between two co-authors if their collaboration relates to the topic of that layer. The Obama dataset [52] captures different types of social interactions (e.g., retweeting, mentioning, replying) on Twitter during Barack Obama's visit to Israel in 2013. The YEAST dataset [52] represents interaction networks of genes in *Saccharomyces cerevisiae*, with layers representing positive interactions, negative interactions, positive correlations, or negative correlations. The Higgs dataset [52] contains four layers, each representing a type of Twitter interaction: friendship, replying, mentioning, or retweeting. In the StackOverflow dataset [44], layers represent user connections within specific years. The Wiki dataset [30] contains users and pages from Wikipedia, where layers correspond to yearly edit events. Lastly, the MAG dataset [22], derived from the MAG240M graph in OGB-LSC [22], has layers representing citations of papers within specific years.

C SUPPLEMENTARY EXPERIMENTAL RESULTS

This section presents additional experimental results that are not included in the main text.

Exp-1: Community quality comparison for different models under default parameters.

Parameter settings. The baselines include d -CC, FirmCore, FocusCore, CrossCore, k -core, $(k+1)$ -core in the projected graph, and FirmTruss. First, all these baselines have the parameter k . Hence, the parameter k is set to the same value for all models on the same multilayer graph. For the k -core, setting the same k for layers may result in an empty result. Thus, we set each $k_i \in \mathbf{k}$ to the largest possible value that satisfies $k_i \leq k$. Second, some models have additional parameters, which are set separately. Specifically, we set a specific s value for SynCore and assign $\lambda = s$ for both FirmCore and FirmTruss. For d -CC and FocusCore, we select the top s densest layers as the target layers for community search.

Table 4 shows the results for all datasets. SynCore achieves the best performance across all metrics due to its requirement for cohesive community structures both within individual layers and in the projected graph. This enables SynCore to identify highly cohesive communities. Other models like d -CC, CrossCore, and extbfk-core only consider cohesiveness within partial layers, resulting in lower densities and clustering coefficients compared to SynCore. FirmCore and FirmTruss do not require dense structures across layers, leading to lower-quality communities. FocusCore, which combines d -CC and FirmCore, does not significantly enhance community quality. The $(k+1)$ -core in the projected graph performs the worst, showing that the quality of SynCore is not solely reliant on projected graph constraints. These results support the effectiveness of SynCore’s design.

Exp-2: Community quality comparison for different models under optimal parameters. Table 5 shows the performance of all models under their optimal hyperparameter settings. Overall, SynCore demonstrates superior quality compared to other models in most cases. In rare instances, SynCore performs slightly worse on certain metrics. For example, FirmTruss outperforms SynCore on the $GCC-P$ metric in the DB dataset. This is because FirmTruss focuses on finding triangle-containing structures, which enhances the $GCC-P$ metric. For large graphs, such as the WK and MG datasets, evaluations of FocusCore, k -core, and FirmTruss could not be completed within 24 hours. Therefore, their results are not reported. For FocusCore and k -core, the excessive number of parameter combinations led to an extremely long computation time, making it infeasible to complete within the given timeframe. For FirmTruss, the high computational complexity, due to its intricate structure, resulted in an excessively long computation time, preventing completion within the time limit.

Exp-3: Effect of k on community quality. We explore the effect of parameter k on community quality. Figure 17 show the results. As k increases, all metrics consistently improve. This is because a higher k results in more neighbors, which enhances the cohesiveness of the community. With a larger k , each vertex in the community is connected to more nodes, thereby increasing both the density and the global clustering coefficient (GCC) of the community structure.

Exp-4: Effect of s on community quality. We explore the effect of parameter s on community quality. Figure 18 show the results. Increasing s improves the quality of the resulting communities. Larger s values require more layers to meet cohesiveness, leading to more refined community structures. As s increases, the requirement for cohesion across multiple layers becomes stricter, which helps in filtering out loosely connected vertices and retaining only the most cohesive parts of the community. This ultimately results in communities that are more strongly interconnected and exhibit higher quality metrics.

Exp-5: Effect of $|Q|$ on community quality. We explore the effect of parameter $|Q|$ on community quality. Figure 19 show the results. Metrics are unaffected by the number of query vertices. SynCS returns the largest SynCore, meaning the resulting vertices are not directly influenced by $|Q|$.

Exp-6: Effect of k on search time. First, we explore the effect of parameter k . Figure 20 show the results. We have the following observations. (1) DSA demonstrates the best performance among the three algorithms, being up to six orders of magnitude faster than BM. Additionally, PSA is up to three orders of magnitude faster than BM. DSA achieves the best performance because it uses the DLT index to store the precomputed SynCore decomposition results, avoiding multiple traversals of multilayer graphs. In contrast, BM must enumerate all layer combinations and use the peeing technique to find the SynCore for each layer combination, resulting in the worst performance. (2) As k increases, the search time of DSA decreases, while the search times of PAS and BM remain almost unchanged. It is because the larger k , the smaller SynCore. Thus, DSA traverses fewer DLT nodes to find SynCore, reducing the search time. For PSA and BM, the parameter k does not influence the number of layer combinations. Hence, their search times almost keep the same.

Exp-7: Effect of s on search time. Next, we study the effect of s . The results are shown in Figure 21. First, the search time of the DSA decreases as s increases. This is because a larger s results in a smaller SynCore, reducing the search space in the DLT index. Second, as s increases, the number of layer combinations also increases, causing BM to take more time. Third, although a larger s leads to more layer combinations, PSA can prune these layer combinations to a small number, resulting in stable performance. Both DAS and PSA consistently outperform BM across different values of s .

Exp-8: Effect of $|Q|$ on search time. Then, we test the effect of the number of query vertices by varying $|Q|$ from 1 to 8. The results are shown in Figure 22. As the number of query vertices increases, the search times for DSA and PSA slightly decrease, while the search time for BM shows no obvious change. For DSA and PSA, more query vertices lead to fewer layer combinations, accelerating the search process. In contrast, BM needs to compute SynCore for all layer combinations, whose number does not change for different $|Q|$ values. Hence, the number of query vertices does not significantly affect BM’s search time.

Exp-9: Effect of $|L|$ on search time. In this experiment, we vary the number of layers in the multilayer graphs and evaluate the performance of three algorithms. The results are shown in Figure 23. We observe that as $|L|$ increases, the performance of all algorithms deteriorates. This is because more layers in the multilayer graphs

Table 4: Community quality comparison for different models (default parameters)
(Metrics: ①: *D-Avg*, ②: *D-Min*, ③: *D-P*, ④: *GCC-Avg*, ⑤: *GCC-Min*, ⑥: *GCC-P*)

Datasets	SD ($k = 3, s = 2$)						HM ($k = 10, s = 2$)						SC ($k = 20, s = 2$)						DB ($k = 15, s = 2$)						OB ($k = 15, s = 3$)					
Metrics	①	②	③	④	⑤	⑥	①	②	③	④	⑤	⑥	①	②	③	④	⑤	⑥	①	②	③	④	⑤	⑥	①	②	③	④	⑤	⑥
SynCore	0.50	0.41	0.53	0.24	0.24	0.34	0.47	0.45	0.64	0.83	0.80	0.85	0.55	0.51	0.56	0.85	0.80	0.90	0.41	0.41	0.45	0.71	0.70	0.73	0.46	0.44	0.50	0.48	0.46	0.51
d-CC	0.28	0.25	0.35	0.14	0.14	0.20	0.31	0.30	0.46	0.67	0.40	0.68	0.44	0.40	0.48	0.80	0.76	0.81	0.30	0.29	0.40	0.61	0.60	0.64	0.35	0.33	0.42	0.41	0.38	0.47
FirmCore	0.00	0.00	0.00	0.01	0.01	0.01	0.00	0.00	0.01	0.06	0.01	0.07	0.00	0.00	0.02	0.08	0.05	0.10	0.00	0.00	0.00	0.04	0.03	0.05	0.00	0.00	0.01	0.02	0.02	0.03
FocusCore	0.35	0.31	0.38	0.17	0.16	0.24	0.39	0.34	0.53	0.78	0.71	0.79	0.44	0.40	0.48	0.80	0.76	0.81	0.38	0.36	0.42	0.69	0.68	0.70	0.41	0.39	0.44	0.45	0.42	0.48
CrossCore	0.28	0.25	0.35	0.14	0.14	0.20	0.35	0.32	0.51	0.68	0.44	0.73	0.44	0.42	0.48	0.82	0.77	0.85	0.30	0.29	0.40	0.61	0.60	0.64	0.36	0.33	0.43	0.42	0.39	0.48
k-core	0.29	0.25	0.36	0.15	0.14	0.21	0.39	0.33	0.54	0.68	0.41	0.77	0.47	0.43	0.49	0.83	0.79	0.87	0.31	0.30	0.41	0.62	0.61	0.65	0.36	0.33	0.43	0.42	0.39	0.48
(k+1)-core	0.00	0.00	0.00	0.01	0.00	0.01	0.00	0.00	0.03	0.01	0.05	0.05	0.00	0.00	0.01	0.08	0.05	0.10	0.00	0.00	0.00	0.01	0.01	0.02	0.00	0.00	0.00	0.01	0.00	0.01
FirmTruss	0.11	0.09	0.15	0.10	0.09	0.16	0.06	0.00	0.27	0.34	0.12	0.46	0.09	0.02	0.42	0.39	0.26	0.55	0.10	0.01	0.30	0.51	0.13	0.56	0.13	0.11	0.15	0.20	0.08	0.25

Datasets	YE ($k = 30, s = 3$)						HI ($k = 10, s = 3$)						SO ($k = 20, s = 3$)						WK ($k = 15, s = 3$)						MG ($k = 30, s = 3$)					
Metrics	①	②	③	④	⑤	⑥	①	②	③	④	⑤	⑥	①	②	③	④	⑤	⑥	①	②	③	④	⑤	⑥	①	②	③	④	⑤	⑥
SynCore	0.30	0.20	0.87	0.34	0.20	0.91	0.27	0.22	0.39	0.51	0.43	0.59	0.74	0.68	0.92	0.75	0.74	0.93	0.23	0.19	0.38	0.72	0.61	0.79	0.43	0.38	0.59	0.46	0.37	0.92
d-CC	0.23	0.14	0.76	0.24	0.15	0.81	0.14	0.10	0.22	0.37	0.30	0.46	0.48	0.44	0.72	0.60	0.52	0.81	0.16	0.14	0.29	0.60	0.53	0.71	0.29	0.28	0.37	0.34	0.30	0.66
FirmCore	0.00	0.00	0.00	0.01	0.01	0.02	0.00	0.00	0.00	0.01	0.00	0.02	0.00	0.00	0.00	0.04	0.03	0.23	0.00	0.00	0.00	0.03	0.02	0.05	0.00	0.00	0.00	0.04	0.03	0.05
FocusCore	0.27	0.16	0.78	0.28	0.17	0.85	0.16	0.12	0.25	0.39	0.33	0.48	0.52	0.48	0.82	0.64	0.62	0.85	0.21	0.18	0.36	0.69	0.61	0.78	0.38	0.35	0.55	0.42	0.36	0.78
CrossCore	0.23	0.14	0.76	0.24	0.15	0.81	0.14	0.10	0.22	0.37	0.30	0.46	0.50	0.46	0.75	0.61	0.53	0.82	0.17	0.15	0.31	0.62	0.55	0.74	0.31	0.29	0.42	0.35	0.31	0.68
k-core	0.23	0.15	0.77	0.25	0.16	0.82	0.14	0.10	0.22	0.40	0.33	0.46	0.52	0.49	0.79	0.66	0.63	0.84	0.17	0.15	0.31	0.63	0.56	0.74	0.34	0.33	0.50	0.40	0.36	0.76
(k+1)-core	0.00	0.00	0.00	0.01	0.00	0.01	0.00	0.00	0.00	0.00	0.01	0.29	0.00	0.00	0.00	0.02	0.01	0.29	0.00	0.00	0.00	0.01	0.01	0.02	0.00	0.00	0.00	0.01	0.01	0.02
FirmTruss	0.10	0.06	0.24	0.19	0.10	0.28	0.05	0.00	0.14	0.16	0.08	0.34	0.19	0.01	0.69	0.56	0.21	0.81	0.10	0.01	0.27	0.38	0.32	0.60	0.10	0.01	0.18	0.25	0.22	0.60

Table 5: Community quality comparison for different models (optimal parameters)
(Metrics: ①: *D-Avg*, ②: *D-Min*, ③: *D-P*, ④: *GCC-Avg*, ⑤: *GCC-Min*, ⑥: *GCC-P*)

Datasets	SD						HM						SC						DB						OB					
Metrics	①	②	③	④	⑤	⑥	①	②	③	④	⑤	⑥	①	②	③	④	⑤	⑥	①	②	③	④	⑤	⑥	①	②	③	④	⑤	⑥
SynCore	0.86	0.65	0.76	0.27	0.26	0.41	0.78	0.73	0.88	0.83	0.81	0.91	0.85	0.70	0.82	0.88	0.86	0.94	0.66	0.60	0.72	0.84	0.73	0.85	0.70	0.67	0.75	0.75	0.66	0.80
d-CC	0.55	0.45	0.58	0.15	0.14	0.21	0.49	0.48	0.67	0.69	0.68	0.81	0.58	0.54	0.59	0.85	0.78	0.86	0.42	0.42	0.61	0.70	0.69	0.71	0.47	0.45	0.59	0.51	0.43	0.54
FirmCore	0.40	0.04	0.44	0.11	0.02	0.15	0.40	0.07	0.54	0.53	0.08	0.63	0.33	0.04	0.48	0.46	0.09	0.68	0.28	0.02	0.45	0.40	0.09	0.54	0.25	0.05	0.53	0.35	0.03	0.39
FocusCore	0.71	0.51	0.61	0.17	0.16	0.28	0.69	0.62	0.75	0.80	0.73	0.83	0.66	0.57	0.62	0.89	0.80	0.92	0.53	0.52	0.64	0.72	0.72	0.79	0.58	0.51	0.60	0.53	0.48	0.54
CrossCore	0.55	0.45	0.58	0.15	0.14	0.21	0.49	0.48	0.67	0.69	0.68	0.81	0.58	0.54	0.59	0.85	0.78	0.86	0.42	0.42	0.61	0.70	0.69	0.71	0.47	0.45	0.59	0.51	0.43	0.62
k-core	0.55	0.46	0.64	0.16	0.16	0.21	0.55	0.48	0.69	0.74	0.72	0.82	0.63	0.59	0.62	0.86	0.81	0.88	0.43	0.43	0.62	0.75	0.72	0.78	0.51	0.47	0.66	0.54	0.47	0.68
(k+1)-core	0.28	0.02	0.30	0.07	0.01	0.12	0.31	0.05	0.42	0.33	0.06	0.49	0.20	0.03	0.30	0.49	0.06	0.49	0.21	0.01	0.31	0.25	0.07	0.33	0.17	0.04	0.34	0.24	0.02	0.26
FirmTruss	0.69	0.18	0.67	0.18	0.11	0.27	0.52	0.09	0.64	0.64	0.16	0.73	0.59	0.22	0.57	0.63	0.32	0.85	0.47	0.06	0.52	0.61	0.20	0.88	0.49	0.18	0.68	0.58	0.15	0.67

Datasets	YE						HI						SO						WK						MG					
Metrics	①	②	③	④	⑤	⑥	①	②	③	④	⑤	⑥	①	②	③	④	⑤	⑥	①	②	③	④	⑤	⑥	①	②	③	④	⑤	⑥
SynCore	0.49	0.37	0.96	0.44	0.27	0.97	0.50	0.43	0.80	0.65	0.55	0.74	0.94	0.93	0.98	0.88	0.77	0.96	0.53	0.40	0.79	0.86	0.71	0.93	0.64	0.45	0.76	0.51	0.40	0.97
d-CC	0.37	0.23	0.81	0.36	0.20	0.84	0.41	0.30	0.71	0.42	0.36	0.55	0.74	0.68	0.92	0.62	0.56	0.83	0.37	0.34	0.73	0.72	0.63	0.79	0.44	0.38	0.60	0.39	0.36	0.79
FirmCore	0.30	0.03	0.51	0.30	0.02	0.62	0.24	0.03	0.47	0.25	0.03	0.33	0.57	0.04	0.63	0.35	0.03	0.78	0.28	0.02	0.57	0.47	0.04	0.69	0.32	0.05	0.35	0.31	0.03	0.63
FocusCore	0.44	0.27	0.82	0.41	0.27	0.85	0.46	0.37	0.81	0.46	0.41	0.55	-	-	-	-	-	-	-	-	-	-	-	-	-	-	-	-	-	-
CrossCore	0.37	0.23	0.81	0.36	0.20	0.84	0.41	0.30	0.71	0.42	0.36	0.55	0.74	0.68	0.92	0.62	0.56	0.83	0.37	0.34	0.73	0.72	0.63	0.79	-	-	-	-	-	-
k-core	0.39	0.24	0.86	0.39	0.20	0.95	0.42	0.31	0.73	0.43	0.36	0.59	-	-	-	-	-	-	-	-	-	-	-	-	-	-	-	-	-	-
(k+1)-core	0.22	0.02	0.49	0.20	0.01	0.40	0.16	0.02	0.29	0.18	0.02	0.20	0.37	0.03	0.41	0.27	0.02	0.58	0.22	0.02	0.45	0.28	0.03	0.50	0.20	0.03	0.34	0.20	0.02	0.47
FirmTruss	0.37	0.10	0.88	0.41	0.12	0.72	0.41	0.06	0.70	0.36	0.14	0.66	-	-	-	-	-	-	-	-	-	-	-	-	-	-	-	-	-	-

result in more layer combinations, thereby expanding the search space and increasing the search time. Notably, despite the varying number of layers, PSA remains 1 to 2 orders of magnitude faster than BM, while DSA maintains approximately 2 orders of magnitude faster performance than PSA.

Exp-10: Scalability. Finally, we evaluate the scalability of three algorithms under different graph sizes. In this experiment, we randomly sample a certain number of vertices from the original graph to generate a set of graphs with different cardinalities. Results are shown in Figure 24. As expected, the performance of all algorithms degenerates when the graph cardinality increases. The reason is that the larger the graph, the larger the community. However, DSA and PSA consistently outperform BM by several orders of magnitude.

Exp-11: DLT Maintenance. Finally, we evaluate the performance of DLT maintenance by randomly inserting and removing different numbers of edges, ranging from 2^0 to 2^{10} . The maintenance times are shown in Figure 26. *DLT-Ins* and *DLT-Rm* denote the

maintenance algorithms for edge insertion and removal, respectively. *Rebuild* denotes to build the index from scratch whenever the multilayer graphs update. We have two key observations. First, both *DLT-Ins* and *DLT-Rm* are more efficient than *Rebuild*. Second, the performance of both *DLT-Ins* and *DLT-Rm* degenerate as the number of inserted/removed edges

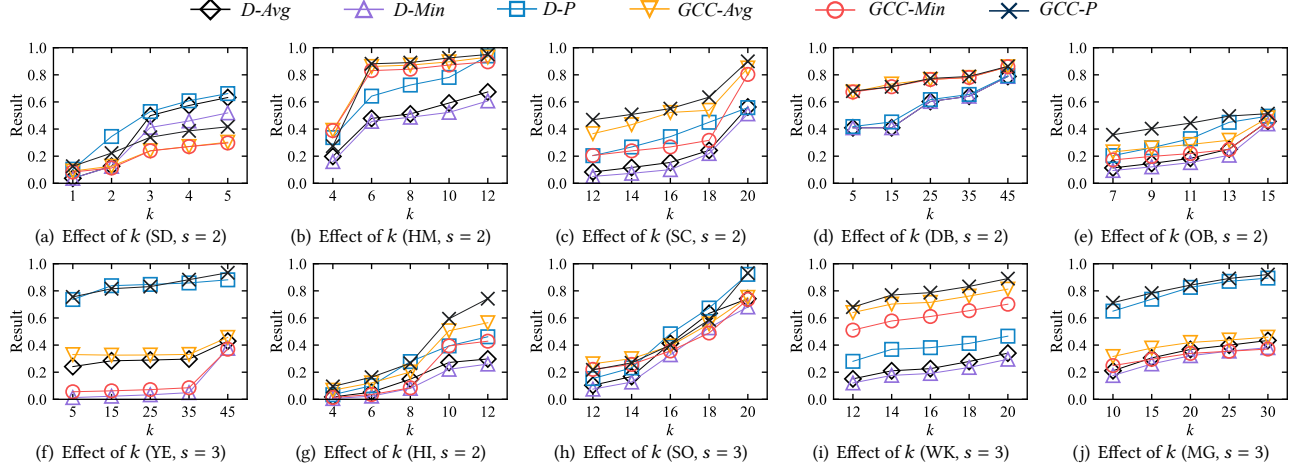


Figure 17: Effect of k on community quality

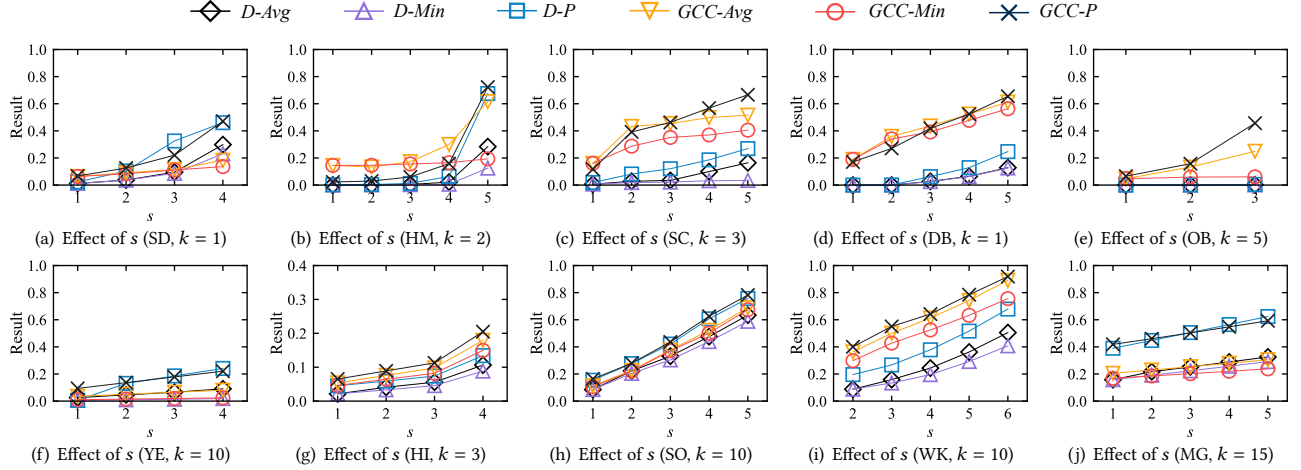


Figure 18: Effect of s on community quality

Exp-13: Effect of $|L|$ on DLT. Next, we vary the number of layers in the datasets to test the performance of DLT. To this end, we randomly select a certain number of layers to generate multilayer graphs with different layer counts. The index size and construction time are shown in Figure 27. As the number of layers increases, both the index size and construction time increase. This is because as the number of layers increases, the number of non-empty SynCores will also increase, leading to more dominant layers. Essentially, the index stores all dominant layers, so DLT becomes larger and takes more time to construct. However, the index size of DLT is consistently comparable to the graph size. Additionally, since DLT builds on the results of the SynCore decomposition, its construction time remains a small fraction of the total build time.

Exp-14: Ablation Study. In Tables 6-7, we present a detailed comparison of the quality and size of communities obtained with and without global cohesiveness. The results clearly show that SynCore with global cohesiveness significantly outperforms the version without it in terms of community quality. The inclusion of global cohesiveness ensures that the identified communities are more cohesive. Moreover, global cohesiveness effectively eliminates a considerable number of irrelevant vertices that would otherwise dilute the community. This pruning process results in smaller, more focused communities that better capture the underlying structure of the graph. These findings demonstrate that global cohesiveness is both essential and non-redundant, as it plays a crucial role in improving community quality while maintaining tighter and more compact structures.

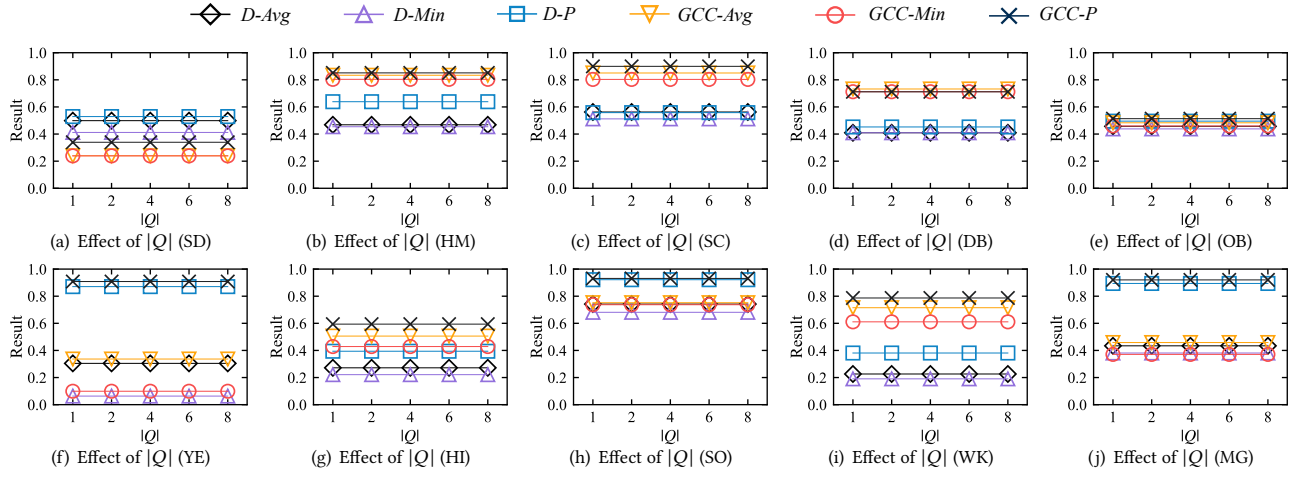


Figure 19: Effect of $|Q|$ on community quality

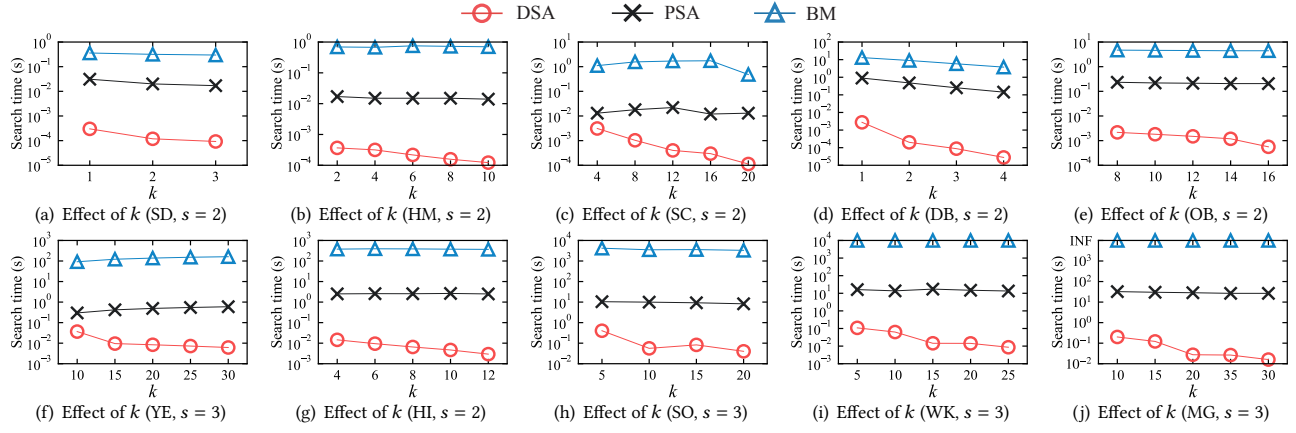


Figure 20: Effect of k on search algorithms

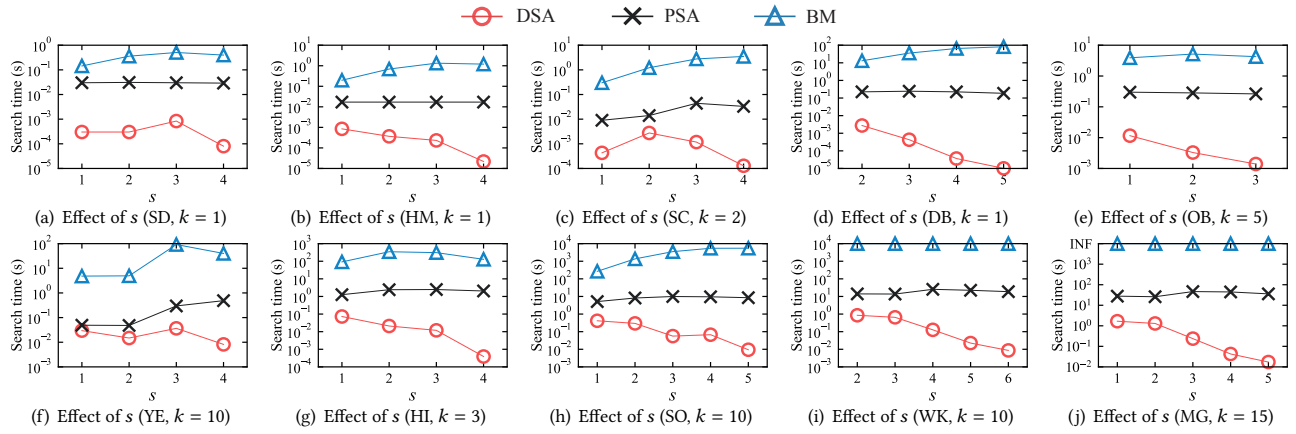


Figure 21: Effect of s on search algorithms

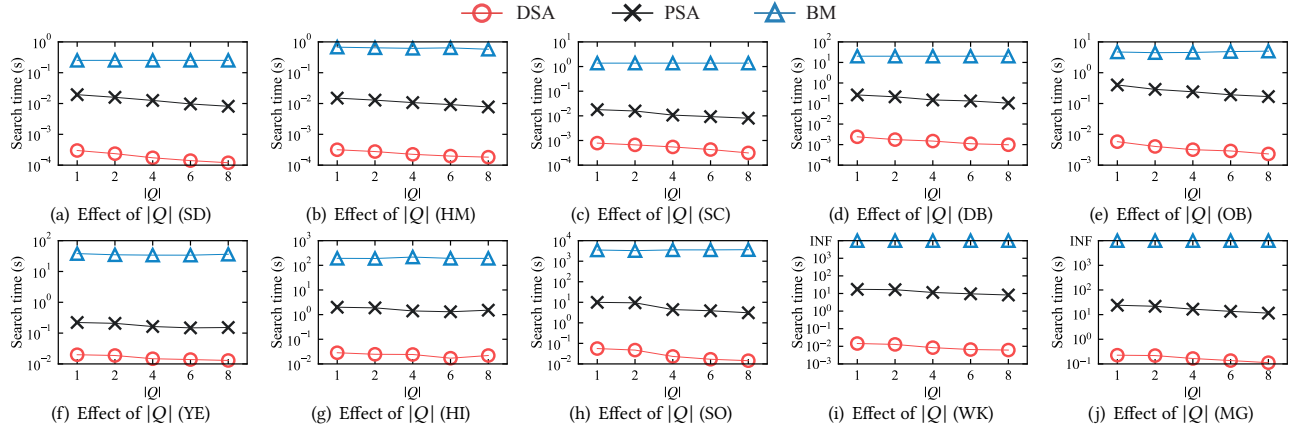


Figure 22: Effect of $|Q|$ on search algorithms

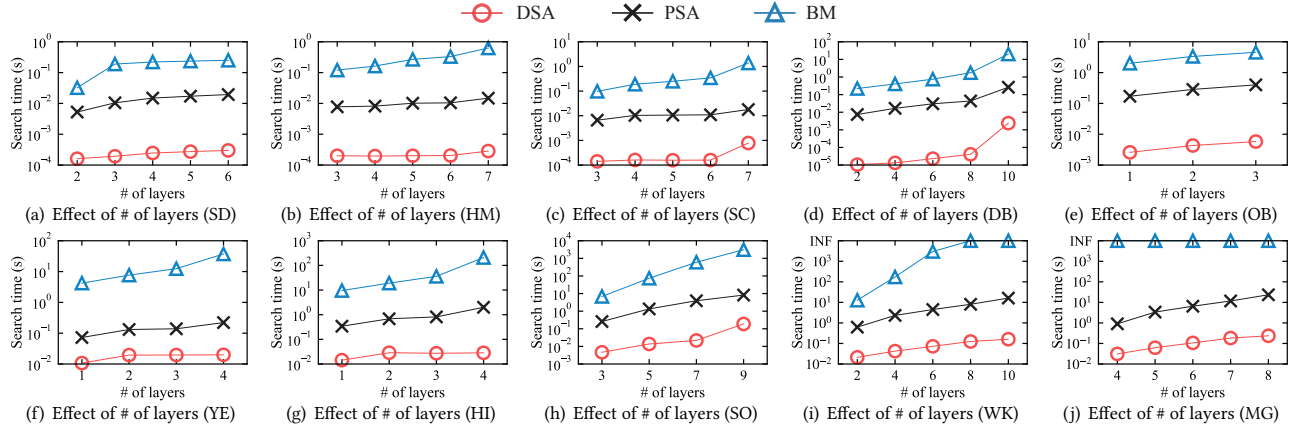


Figure 23: Effect of # of layers on search algorithms

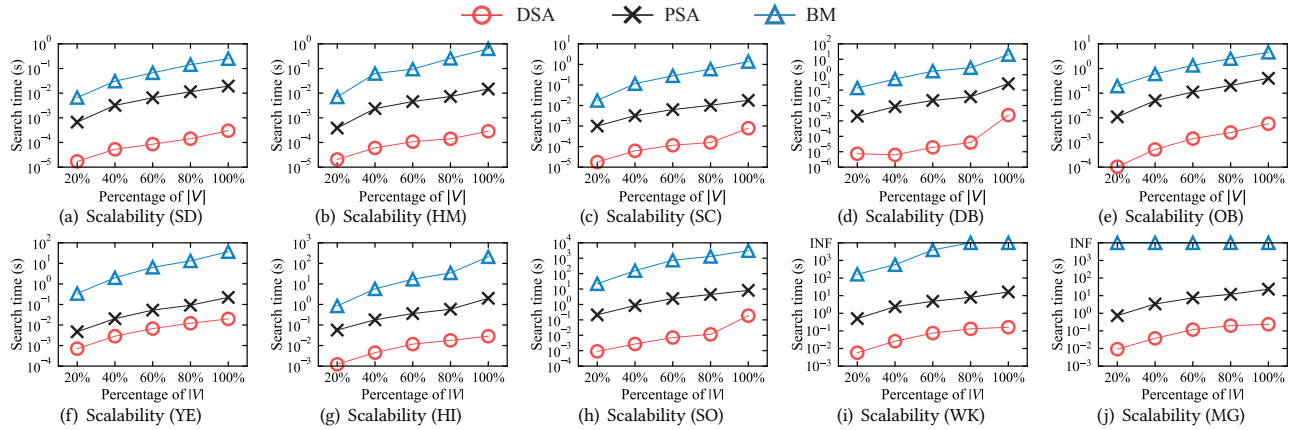


Figure 24: Scalability on search algorithms

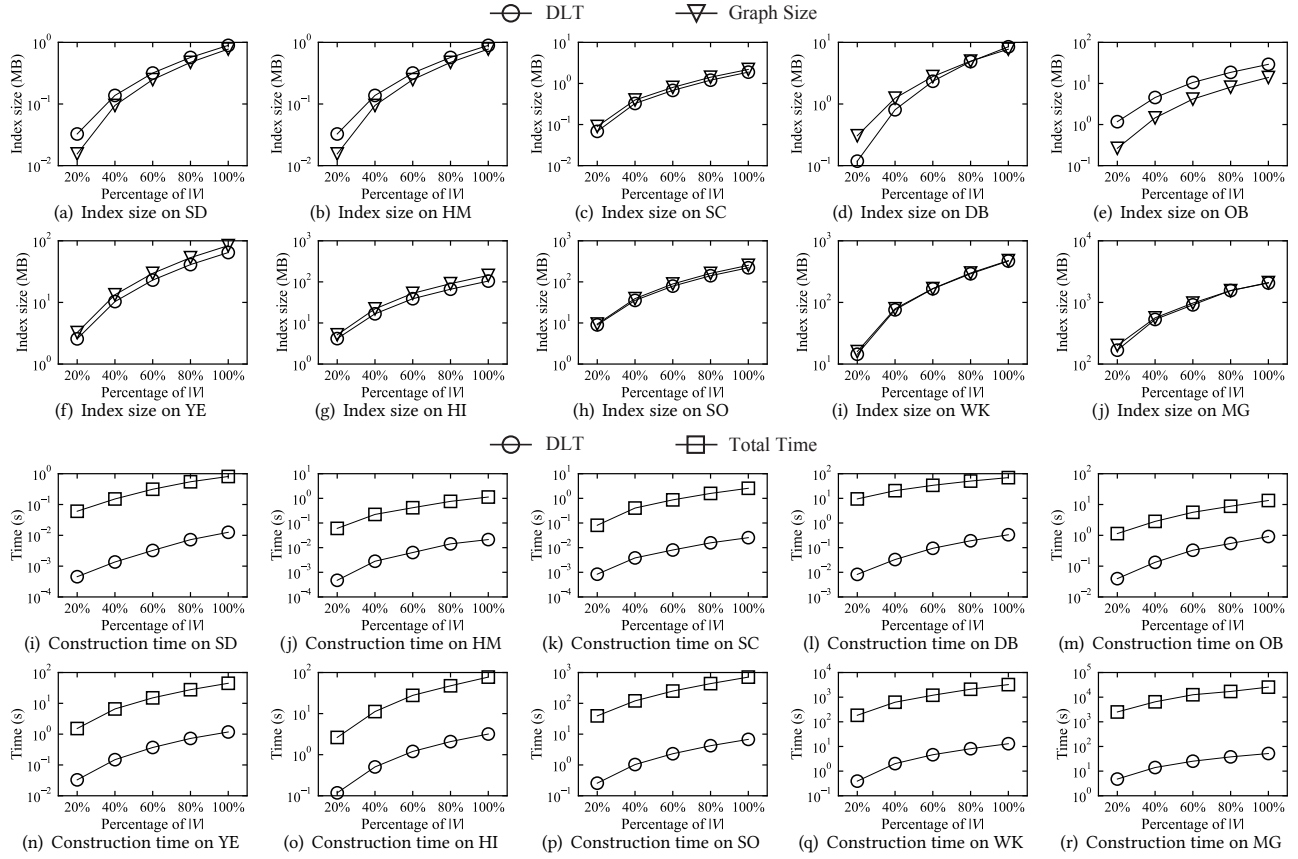


Figure 25: Scalability on DLT

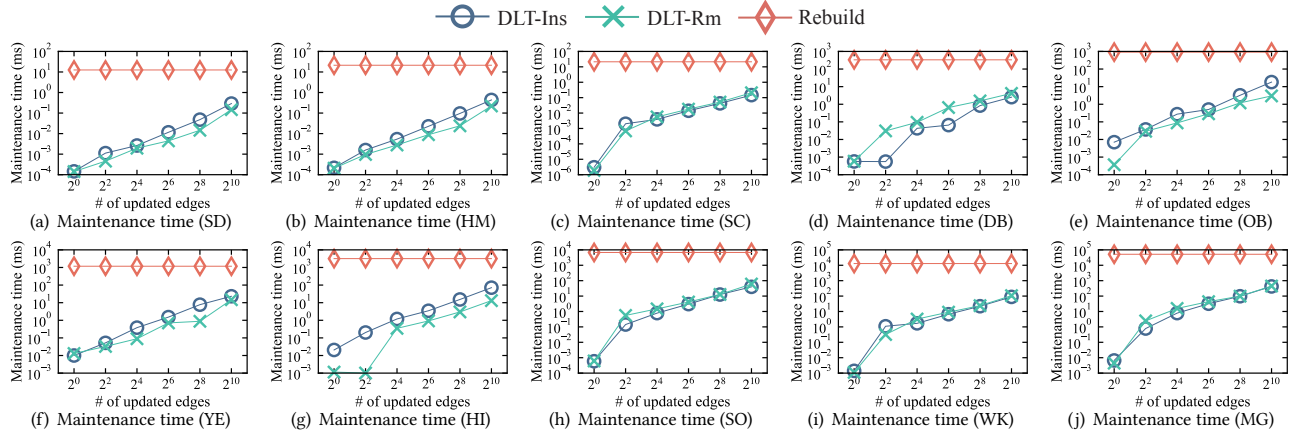


Figure 26: DLT maintenance

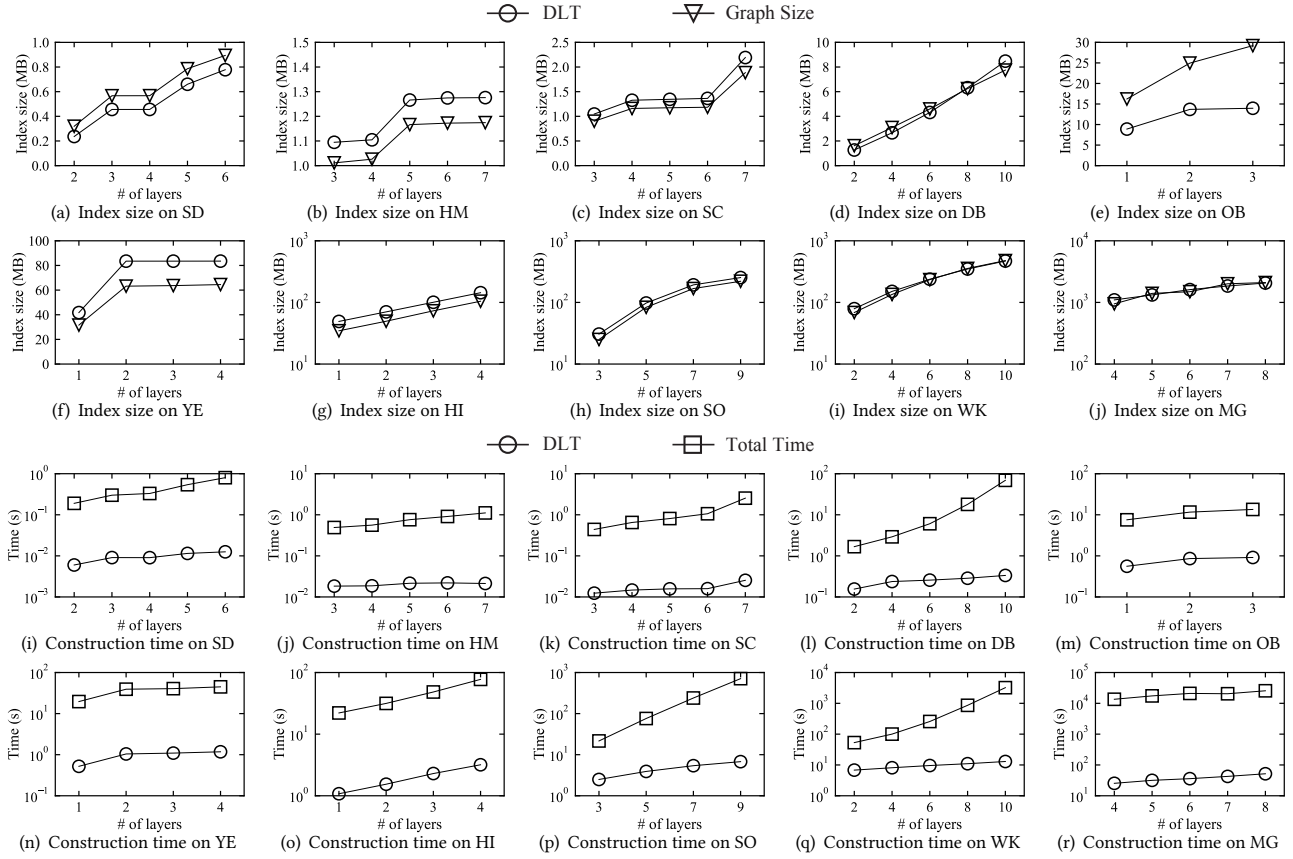


Figure 27: Effect of # of layers on DLT

Table 6: Community quality comparison for SynCore with and without global cohesivness (default parameters)
(Metrics: ①: *D-Avg*, ②: *D-Min*, ③: *D-P*, ④: *GCC-Avg*, ⑤: *GCC-Min*, ⑥: *GCC-P*)

Datasets	SD ($k = 3, s = 2$)						HM ($k = 10, s = 2$)						SC ($k = 20, s = 2$)						DB ($k = 15, s = 2$)						OB ($k = 15, s = 3$)					
Metrics	①	②	③	④	⑤	⑥	①	②	③	④	⑤	⑥	①	②	③	④	⑤	⑥	①	②	③	④	⑤	⑥	①	②	③	④	⑤	⑥
SynCore	0.50	0.41	0.53	0.24	0.24	0.34	0.47	0.45	0.64	0.83	0.80	0.85	0.55	0.51	0.56	0.85	0.80	0.90	0.41	0.41	0.45	0.73	0.71	0.71	0.46	0.44	0.50	0.48	0.46	0.51
SynCore w/o global	0.25	0.22	0.33	0.12	0.11	0.17	0.28	0.25	0.41	0.56	0.39	0.65	0.44	0.40	0.48	0.80	0.76	0.81	0.30	0.29	0.40	0.61	0.60	0.64	0.29	0.28	0.38	0.38	0.36	0.44
Datasets	YE ($k = 30, s = 3$)						HI ($k = 10, s = 3$)						SO ($k = 20, s = 3$)						WK ($k = 15, s = 3$)						MG ($k = 30, s = 3$)					
Metrics	①	②	③	④	⑤	⑥	①	②	③	④	⑤	⑥	①	②	③	④	⑤	⑥	①	②	③	④	⑤	⑥	①	②	③	④	⑤	⑥
SynCore	0.30	0.20	0.87	0.34	0.20	0.91	0.27	0.22	0.39	0.51	0.43	0.59	0.74	0.68	0.92	0.75	0.74	0.93	0.23	0.19	0.38	0.72	0.61	0.79	0.43	0.38	0.59	0.46	0.37	0.92
SynCore w/o global	0.23	0.14	0.76	0.24	0.15	0.81	0.13	0.08	0.22	0.31	0.26	0.39	0.43	0.42	0.71	0.53	0.42	0.71	0.14	0.13	0.28	0.54	0.50	0.61	0.26	0.24	0.35	0.32	0.27	0.54

Table 7: Community size comparison for SynCore with and without global cohesivness (default parameters)
(The numbers represent # of vertices in the community)

Datasets	SD ($k = 3, s = 2$)	HM ($k = 10, s = 2$)	SC ($k = 20, s = 2$)	DB ($k = 15, s = 2$)	OB ($k = 15, s = 3$)	YE ($k = 30, s = 3$)	HI ($k = 10, s = 3$)	SO ($k = 20, s = 3$)	WK ($k = 15, s = 3$)	MG ($k = 30, s = 3$)
SynCore	10	26	46	42	40	173	51	35	89	88
SynCore w/o global	19	49	63	65	64	261	145	58	145	147